Advances in the development of dielectric elastomer generators for wave energy conversion

Advances in the development of dielectric elastomer generators for wave energy conversion

Giacomo Moretti[1,2], Miguel Santos-Herran[3], David Forehand[3], Marco Alves[4], Henry Jeffrey[3], Rocco Vertechy[5], and Marco Fontana[2]

[1]TeCIP Institute, Scuola Superiore Sant'Anna, Pisa, Italy
[2]Department of Industrial Engineering, University of Trento, Italy
[3]Institute for Energy Systems, The University of Edinburgh, UK
[4]WaveEC Offshore Renewables, Lisbon, Portugal
[5]Department of Industrial Engineering, University of Bologna, Italy

Abstract

This paper presents a summary of recent progresses towards the development and upscaling of an emerging class of electrostatic power take-off systems for wave energy converters (WECs), called dielectric elastomer generators (DEGs). DEGs are electromechanical devices able to convert mechanical energy into electrical energy by exploiting the deformation of rubber-like dielectric materials. The high power density (in the order of hundreds of Watts per kilogram), good efficiency and ease of assembling combined with the low-cost of the employed materials (a few euros per kilogram) and their intrinsic resilient/reliable response to mechanical shocks make DEGs a very promising option for the deployment of a future generation of WECs.

In the last decade, some specific concepts of WECs based on DEGs have been devised and a remarkable interest in the topic has been aroused in the wave energy community. Among the candidate DEG topologies for wave energy harvesting, recent studies have suggested that a specific layout, namely the axial-symmetric inflating DEG diaphragm, could be a very promising candidate for future upscaling.

This paper first describes the operating principle of DEG PTOs and the effect of electromechanical material parameters on the energetic performance. With reference to the above-mentioned inflating DEG diaphragm topology, an overview of concepts for integration on WECs is then provided, with a special focus on advanced concepts enabling the achievement of dynamical tuning with the incoming waves. A general lumped-parameter modelling approach for the design of DEG-based WECs is proposed. Experimental activity carried out to date, i.e. dry-run laboratory tests, wave-tank tests and preliminary sea trials, is reviewed, with the aim of showing the progression in the devices scale and performance. Finally, economical and technological considerations are outlined, in order to point out challenges, future research opportunities and to draft a roadmap for future research and technological transfer.

1 Introduction

Sea waves are an extraordinarily abundant source of renewable energy, virtually capable of covering a large share of the current worldwide electrical energy demand [1]. Over the last forty years, a

very large number of wave energy converter (WEC) concepts have been proposed, many of which have been built and sea tested, hitting, in a few cases, the target of full-scale deployment and grid-connection [2]. Despite the huge interest in the topic, to date, wave energy has not yet passed the stage of pre-commercial demonstration. Up until now, the high capital cost of marine structures and the difficulty of building devices able to survive in the harsh and aggressive marine environment have prevented WEC technology from becoming economically feasible. In this context, recent actions have been undertaken in order to support research toward "disruptive" solutions, capable of promoting a breakthrough in the wave energy market [3].

Among the proposed game changing solutions, it has been suggested that the technology of dielectric elastomers (DEs), which has its roots in the field of robotics [4], might be successfully transferred to the wave energy sector. DEs are rubber-like dielectrics which can be used to build electrostatic generators, namely DE generators (DEGs), exploiting cyclical deformation-driven capacitance variations to convert mechanical energy into electrical energy [5]. DEs could be employed to implement one of the most critical components of a WEC, i.e., the power take-off (PTO) system. Compared to traditional PTOs, DEGs are potentially cheaper (raw polymeric materials cost a few euros per kilogram), have no moving parts except for the deforming polymeric unit, are corrosion resistant, and potentially feature large conversion efficiency over a wide range of operating frequencies. It has been experimentally proven that, at the operating frequencies of sea waves ($\simeq 10^{-1}$ Hz), DEGs can convert power densities in the order of tens/hundreds of Watts per kilogram of dielectric material, with measured peaks over 200 W/kg [6, 7]. In [7] it is suggested that, assuming an operating power density of just 2 W/kg, the cost of energy of a DEG-based WEC could be reduced to one third of that of conventional WECs.

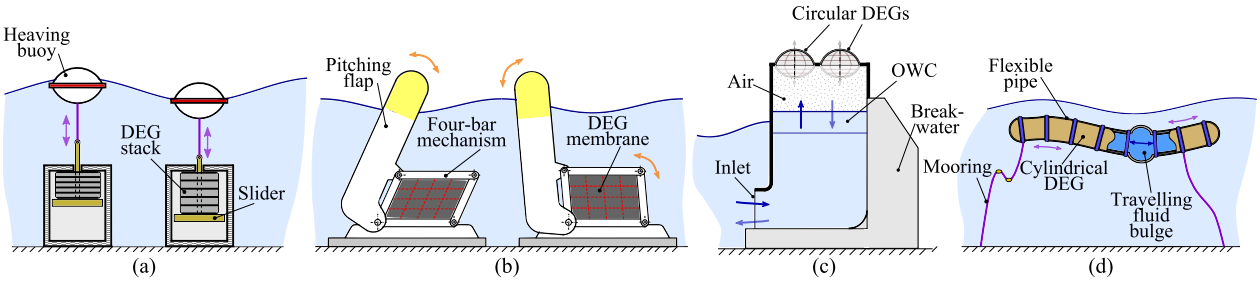

Figure 1: Relevant architectures of WECs with DEG PTOs. (a) Heaving buoy with DEG stack; (b) Pitching flap with framed DEG; (c) Oscillating water column with inflating circular DEG; (d) Bulge wave WEC with cylindrical DEG.

The promising potential performance and the flexibility in terms of layout make DEGs particularly attractive for application on several wave energy converters. New WEC concepts based on DEG PTOs have been devised and investigated by companies and research groups [7–9]. An overview of possible DEG-based WEC concepts proposed in the past is shown in Fig. 1.
Most concepts have been devised by replacing the traditional PTO systems in existing WECs. The modified WECs typically have a primary interface consisting of a floating body, coupled with a DEG PTO. Fig. 1a shows a concept of a floating point absorber connected, through its mooring line, to a pre-compressed stack of DE layers. The cyclical deformation of the stacked DEG is induced by the heaving motion of the floater. This concept has been proposed by Bosch GmbH in the context of the German project EPoSil [10]. A similar concept has been patented by SBM offshore, using a buoyant pitching flap as the primary mover [11]. Such a system, shown in Fig. 1b, can be combined with different DEG architectures, e.g., DEG membranes clamped to the links of a mechanism, as studied in [12]. The primary hydrodynamic interface can be alternatively composed of a fluid vol-

ume oscillating within a collector. This principle is embodied by the device in Fig. 1c, which is an oscillating water column (OWC) [13] with a set of circular inflating DEGs on top of a closed air chamber. This concept, first proposed by Bosch [14], has been recently the object of several studies [15–17], as discussed later in this paper. Finally, it has been suggested that DEGs might be particularly suitable for implementing bulge wave WECs, in which a fluid bulge, originated by local wave pressure, propagates along a rubber-like tubular structure, causing its deformation (see Fig. 1d). SBM Offshore has developed a bulge wave WEC, called the S3, made of a set of inflating tubular DEG segments, functioning both as the structural interface and the PTO [9].

Recently, some research groups, active in the topics of WECs and DEs, joined their efforts towards the creation of a structured scientific investigation into the topic of DEGs for wave energy application. The group explored the numerical and physical modelling, and possible routes towards upscaling and market development of WECs with DEGs [12, 15–17]. This research was initiated under the framework of the EU project PolyWEC [18] and advanced in the context of successive projects, i.e., the WETFEET project [19] and the Wave Energy Scotland initiative [20]. Compared to previous research, which aimed at the development of specific devices and DEG-WEC architectures, the above projects applied a more structured approach to study DEG-based WECs. Starting from the evaluation of several of the concepts discussed above (Fig. 1), attention was progressively focused onto concepts using a particular topology of the DEG PTO, i.e., the circular inflating DEG [15]. Such a topology offers potential integration in WEC devices (see, e.g., Fig. 1c) that are free from rigid moving parts (in contrast to the concepts in Fig. 1a-b) while still relying on existing WEC architectures for which operational experience is available (in contrast with the concept in Fig. 1d).
The research carried out in the context of these initiatives drove, for the first time, the interest of a wide portion of the wave energy community towards the topic of DEGs [3]. Following that, DEGs are now recognised as a potentially disruptive technology for the future of wave energy, with international research and funding agencies, such as Wave Energy Scotland and the European Community, citing them as a strategic topic for future research on WECs [21, 22].

This article presents a review of the tools, findings and goals achieved in the context of recent research on DEG PTO systems for wave energy conversion. A broad view on the problems of selecting suitable materials for DEG PTOs, modelling, and designing DEG-based WEC concepts is provided, and a reflection on the current technological status and future challenges for DEGs is drawn.

The paper is structured as follows. Sect. 2 introduces the operating principle of DEGs and the material requirements for PTO systems design. Sect. 3 describes the topology of the circular diaphragm DEG PTO and its applications on different WEC architectures. Sect. 4 proposes a new general approach for design-oriented physical modelling of DEG-WEC systems. Sect. 5 reviews experimental deployments of scaled DEG prototypes and coupled DEG-WEC systems. Sect. 6 draws a discussion on the current technological state of DEGs, including the effect of technological and operational parameters on the economical competitiveness, and the challenges involved in DEGs future developments. Finally, Sect. 7 presents the conclusions. The paper includes an Appendix which illustrates the application of the proposed modelling approach to two DEG-WEC architectures.

2 DEG operating principle and relevant material properties

This section briefly illustrates the operating principle of DEGs, including a discussion of their operating limits and their high potential as mechanical-to-electrical energy converters in terms of energy/power density. Additionally, the material choice and the relevant physical parameters that

affect the performance of DEGs are addressed.

2.1 Operating principle of a DEG

DEGs are deformable capacitors built by stacking compliant thin DE layers coated with deformable conductive electrodes. The resulting structure is a multilayer membrane made of alternating layers of conductive and non-conductive elastomeric materials. The operating principle of DEGs can be described with reference to a single-layer patch of DE material that is homogeneously stretched along its perimeter and coated with conductive electrodes. The cyclical operation of a DEG [23,24] is schematically represented in Fig. 2a. Specifically, the following four-phases (*P1-P4*) can be identified during operation:

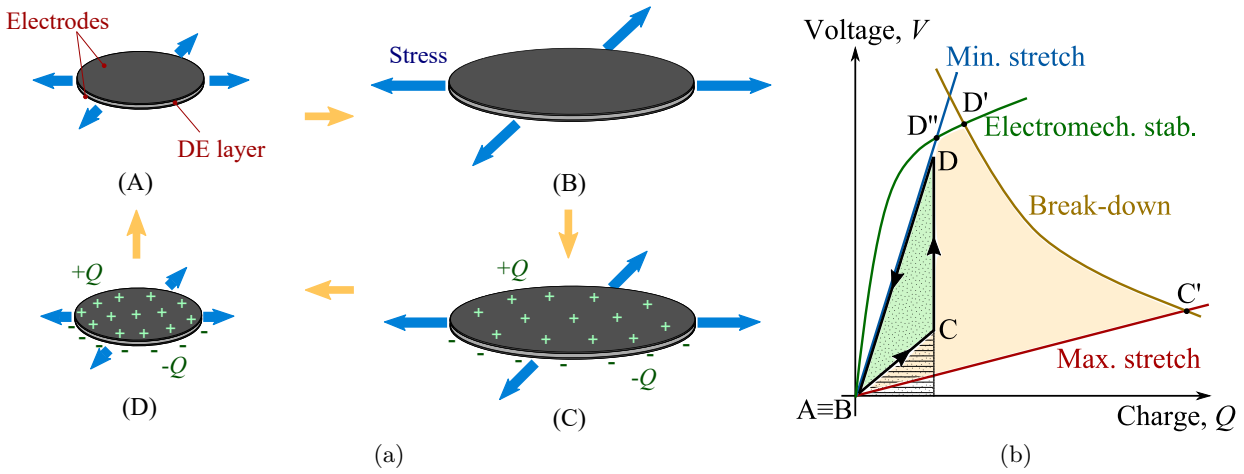

Figure 2: (a) Example of the operating cycle of a DEG. (b) $Q-V$ diagram showing the phases of the DEG operating cycle and the constraints delimiting the feasible working space.

P1 First, as the external load does mechanical work on the DEG, the DEG stretches from configuration (A) (where its capacitance is minimum) to configuration (B) (with increased capacitance), while no charge is present on its electrodes.

P2 Second, as the DEG position (C) is held fixed, a charge Q is deposited on the electrodes. During this phase, called "priming", an amount of electrical energy is initially spent to charge the device.

P3 Third, the external loads take the DEG back to the minimum capacitance configuration (D). During this phase, the charge on the electrodes is assumed to be constant. In this generation phase, the external forces do work against the electrostatic forces, thus causing an increase in the electrostatic energy stored in the DEG.

P4 Finally, in (D), the DEG is fully discharged, and the stored electrostatic energy is recovered.

The described sequence of electro-mechanical transformations can be conveniently represented on a plane whose axes are the DEG charge Q and voltage V [24], as shown in Fig. 2b. The sequence of the phases of the operating cycle is represented by the closed-loop A-B-C-D-A. Straight lines through the axes origin (e.g., B-C, D-A) are iso-capacitance lines, identifying specific DEG geometrical configurations. The amount of energy spent during priming numerically equals the dashed area

subtended below segment B-C, while the energy recovered during DEG discharging equals the dotted area subtended below D-A. The area of the cycle (green area in Fig. 2b) numerically corresponds to the net generated electrical energy.

Although, in the example of Fig. 2a, reference is made to a constant-charge control cycle, the DEG electrical state during phase *P3* can be controlled using different strategies (constant voltage, constant electric field, etc.) [25]. Generic control patterns leading to positive electrical energy generation can be represented as closed counter-clockwise oriented loops on the $Q-V$ diagram. The maximum electrical energy that can be converted in a cycle depends on the admissible stretch range for the DEG and on the following additional limits [24]: 1) the electrical break-down condition, which sets an upper bound to the admissible electric field across the DE (namely, the break-down electric field, E_{BD}) ; 2) electro-mechanical instabilities, which initiate when positive-feedback deformation-voltage variation patterns arise [26]. Such constraints are represented by appropriate curves on the $Q-V$ diagram (see Fig. 2b). The envelope of such limit curves encloses a set of physical states where the DEG can safely operate and it bounds a particular cycle, namely A-B-C'-D'-D"-A in Fig. 2b. It can be demonstrated that the area of such a cycle (yellow area in Fig. 2a) represents the maximum convertible energy and it is proportional to the DE material volume and to the product εE_{BD}^2 [7, 27], where ε is the elastomer dielectric constant.

2.2 Materials

The performance of a DEG, in terms of the convertible energy per cycle, is strongly dependant upon the employed DE material. Specifically, the relevant material properties that affect this figure of merit are:

- Stretchability, which sets the maximum deformation range of the DEG and consequently the obtainable variation in capacitance (represented by the angular range between lines AC' and AD" in Fig. 2b).
- Dielectric constant and break-down electric field, which should be as large as possible to maximise the convertible energy density (see Sect. 2.1).
- Viscoelastic losses (due to material hysteresis) and electric losses (due to non-zero DE conductivity, σ_d).
- Mechanical stiffness: large stiffness leads to large required mechanical loads to deform the DEG, whereas low elastic modulus increases the tendency towards electro-mechanical instabilities [24, 26].

To date, materials employed for DEGs are natural [7] and synthetic [28] rubber, acrylics [6] and silicones [29]. Ranges of the relevant physical properties of the materials are reported in Table 1. In particular, the table shows: shear modulus μ (accounting for the DE elasticity [7]); uniaxial stretch limit, λ_u; hysteresis loss (in uniaxial tensile cycles); dielectric constant ε (normalised by vacuum dielectric constant ε_0); break-down electric field E_{BD}; product εE_{BD}^2; and DE conductivity σ_e.

Acrylic materials (e.g., commercial VHB by 3M) are widely used in laboratory tests [6, 16], due to their low modulus and large dielectric constant, nonetheless, they are unsuitable for industrial use due to their large viscous losses and high conductivity. Natural and synthetic rubber have similar properties (though synthetic rubber seems to perform better in terms of losses), they have large electrical break-down fields, relatively low dielectric constants, and large mechanical stiffnesses. However, silicones seem to be the most promising solution for near-future DEGs. The great

Table 1: Material parameters for some classes of DE.

	Natural rubber [7, 27]	Synthetic rubber [28]	Acrylic [7, 30]	Silicone [31, 32]
Shear modulus, μ (kPa)	500-1000	500-1000	20-50	250-800
Max stretch, λ_u	5-6	5-6	7-9	4-8
Viscous losses (%)	7-20	10-12	15-20	5-10
Relat. dielec. const., $\varepsilon/\varepsilon_0$	2.5-2.8	2.4-2.7	4-4.5	2.5-5
Break-down field, E_{BD} (kV/mm)	100-120	100	70-120	80-150
εE_{BD}^2 (MJ/m^3)	0.22-0.35	0.21-0.24	0.17-0.57	0.14-0.64
Conductivity, σ_d (pS/m)	0.1-1.2	0.1-0.7	1-15	0.1-1.4

advantage of silicone DE sheets relates to their easy-manufacturing and the large potential for the improvement of their relevant material properties through the addition of compounds [29].

Besides DE materials, DEG performance is constrained by the availability of reliable stretchable electrodes. Compliant electrodes can be manufactured using different techniques and materials [33]. Small-scale laboratory prototypes are often made of painted carbon grease [16, 23] or carbon powder [34] electrodes, or hydrogel electrodes [35]. Despite being convenient for experimental tests due to manufacturing simplicity, those solutions do not provide reliable and durable electrodes for real-scale applications. Candidate materials for full-scale electrodes are conductive elastomer layers (doped with conductive carbon particles) or sputtered micrometer-scale thin metallic films [36, 37].

3 The circular diaphragm DEG PTO and its application on WECs

In this section, a particular layout of DEG is presented, which is particularly promising as a PTO for ocean wave energy harvesting, as it can be coupled with different WECs. Such a layout consists of an axial-symmetrical inflating DEG stack, called a circular diaphragm DEG (CD-DEG), and it integrates readily with OWC and pressure differential (PD) devices. A description of the system architecture is presented first; WEC architectures mounting the CD-DEG as the PTO are then introduced, including a mention of relevant design issues.

3.1 Circular diaphragm DEG PTO

The CD-DEG consists of a stack of planar circular DE layers coated by electrodes, clamped along their perimeter to a fixed frame (Fig. 3a). As with rubber-like materials, the CD-DEG stack is incompressible (its volume does not change upon deformation). The stack is mounted on the holding frame with a certain pre-stretch, aimed at preventing loss-of-tension in the presence of electrostatic stresses induced by activation [26]. In particular, indicating with e_0 and t_0 the CD-DEG unstretched radius and thickness respectively, application of an equi-biaxial pre-stretch λ_p takes the DEG stack radius to $e = \lambda_p e_0$ and its thickness to $t_p = t_0/\lambda_p^2$.

CD-DEG operation relies on bubble-like out-of-plane deformations (see Fig. 3b) [15]. When a pressure difference is applied across opposite faces of the CD-DEG, the device inflates (outward or inward, depending on the sign of the pressure difference) and undergoes an increase in the electrodes' surface area, a reduction in thickness and, thus, an increase in capacitance (Fig. 3b).
Consecutive CD-DEG electrodes hold alternating polarity and the different layers of the stack are electrically connected in parallel (Fig. 3a). The partition of the DE material into thin layers allows the limitation of the voltage required to achieve target electric fields. In practice, in order to achieve electric fields in the order of hundreds of kV/mm (see Table 1), output voltages in the

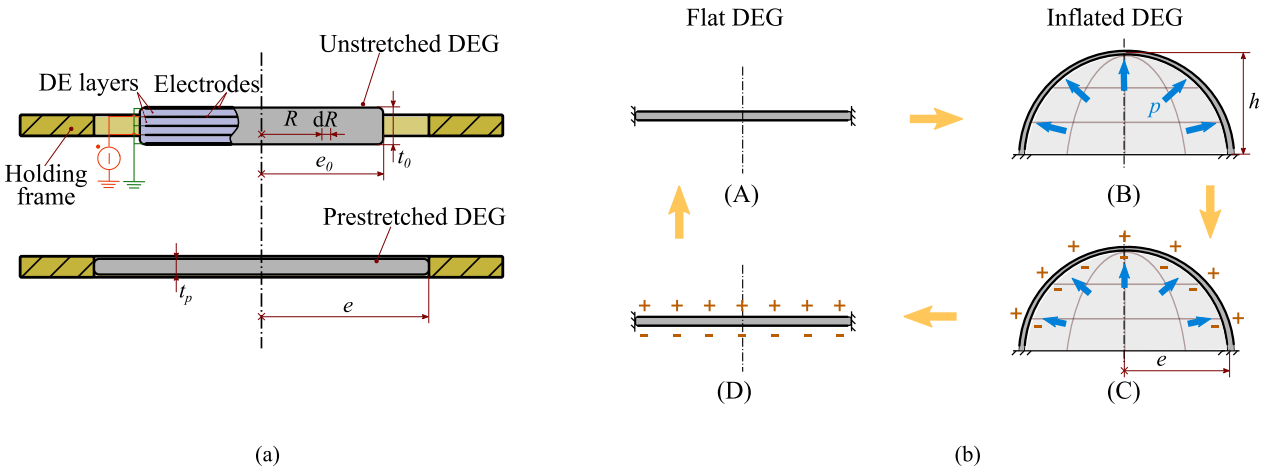

Figure 3: Schematic of the CD-DEG layout and operation. (a) Pre-stretching operation; (b) Operating cycle.

order of tens of kilovolts are required, assuming the use of DE layers with thickness in the order of $\sim 10^{-1}$ mm. Such a value represents a compromise between very large voltages (which would make the power electronics more expensive) and extremely small layer thicknesses (which would make system manufacturing more complicated).

The simplest control cycle for CD-DEGs follows the four-phase logics described in Sect. 2.1. With reference to Fig. 3b, starting from the minimum capacitance (flat) configuration (A), the CD-DEG inflates as a result of the applied pressure difference. The CD-DEG is charged when it reaches the maximally inflated configuration (B-C) (that depends on the external excitation), and it is discharged as it reaches the flat configuration again (C). Such a control cycle only relies on the knowledge of the actual membrane configuration.

3.2 Wave Energy Converters with CD-DEG PTO

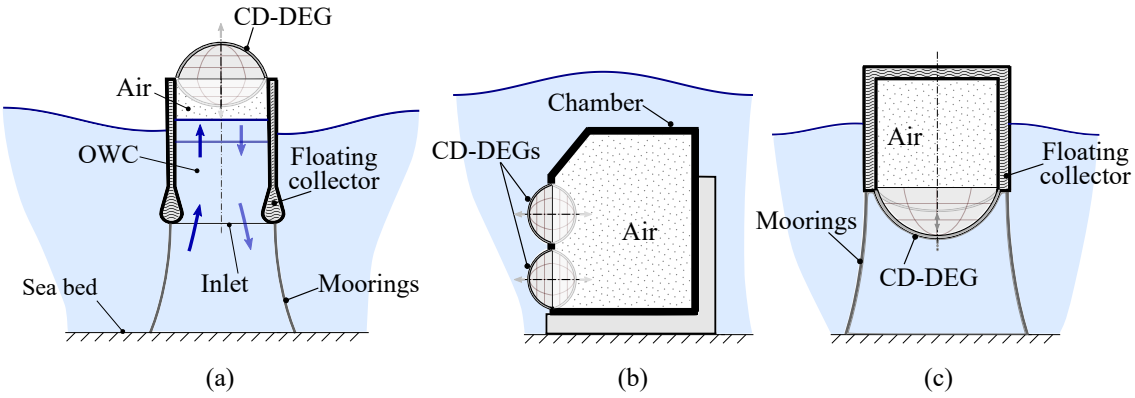

Figure 4: Examples of WECs with CD-DEGs as the PTO system. (a) Floating OWCs; (b) bottom-fixed and (d) floating PD WECs.

The CD-DEG can be employed as the PTO system in different WEC types belonging to two main categories: 1) oscillating water columns (OWCs) mounting the CD-DEG on top of the air chamber (Fig. 1c, 4a), and 2) pressure differential (PD) WECs, in which the CD-DEG is in direct

contact with the sea water (Fig. 4b,c).
OWCs are semi-submerged hollow collectors, open at the bottom towards the sea, and housing a water column which is put into oscillation by the wave induced pressure [13]. Water column oscillations cause the compression/expansion of an air pocket located on top of the OWC. Though OWCs are traditionally equipped with bidirectional air turbines [38], it is possible to employ CD-DEGs as alternative PTO systems. This will potentially overcome the technical issues related to the limited adaptability of the turbines to the harsh sea environment, and their poor efficiency in the presence of bidirectional flows. In OWCs, the air prevents direct contact between the sea water and the DEGs and can be exploited to guarantee DEG safety in rough sea states (e.g., by inducing a quick depressurization through relief valves). OWCs with CD-DEGs have been largely investigated both theoretically [15, 39] and experimentally [16, 17, 40].
PD WECs exploit a submerged interface moved by wave-induced pressure variations. A special PD implementation consists of a hollow chamber filled with a fluid (usually, air) and holding a submerged deformable element (e.g., a polymeric diaphragm) as the hydrodynamic interface [41]. The deformation of that interface induces a pressure variation in the above-mentioned fluid. As in OWCs, such pressure variations can be converted into electricity through turbines or DEGs. However, in PD WECs with CD-DEGs, the DEGs function both as the PTO and the hydrodynamic interface, as their deformation is directly driven by the wave induced pressures. In contrast to OWCs, in which the air chamber compressibility potentially limits the achievable DEG deformation, CD-DEGs combined with PD devices potentially take advantage of larger operating pressure variations and deformations. At the same time, they require greater engineering effort in terms of adaptation of the DEGs to underwater operation.

Both DEG-based OWCs and PD WECs can be implemented as bottom fixed devices (Fig. 1c, 4b), e.g. integrated in break-waters, or as floating moored WECs (Fig. 4a,c). Based on design and manufacturing constraints, the DEG PTO can be potentially implemented as a set of several DEG units installed on a single WEC machine (Fig. 1c, 4b).

3.3 Design of coupled DEG-WEC systems

The design of a WEC with a DEG PTO requires specific consideration of the coupled response of the WEC interface and the DEG. In contrast with other PTO systems, the effect of a DEG is not just that of damping the WEC dynamics. Indeed, its elasticity also plays a relevant role in the system response. The design of an effective DEG-WEC device thus requires an integrated approach, in which the design of the hydrodynamic interface and the DEG is carried out based on their reciprocal influence.

As a matter of fact, the implementation of a DEG PTO involves rather large volumes of DE material. The order of magnitude of the required amount of material for a target application can be calculated based on available estimates of the DEGs' convertible energy density. Theoretical and experimental assessments indicate energy densities in the order of 0.1-1 kJ/kg per cycle [6, 7, 24]. At cyclic operating frequencies equal to typical sea wave frequencies (0.05-0.5 Hz), the mass of DE required to achieve a power output in the order of hundreds of kilowatts (i.e., the typical power target of most full-scale WECs [2]) is thus in the order of tens of tons per WEC unit. Such large DE volumes have an inherent stiffness which supplements the hydrostatic stiffness of the WEC interface, hence influencing the WEC dynamics. In particular, since DEs have strongly non-linear electro-elastic response [26], the DEG PTO introduces a significant non-linearity into the WEC dynamics.

WECs considered in Sect. 3.2 typically feature small dimensions compared to the wavelengths of ocean waves, i.e., they behave as point absorbers [42]. For point absorbing WECs with linear

dynamical response, the maximum power transfer from the waves to the PTO takes place in resonance conditions, i.e., when the natural frequency of the system matches the frequency content of the incoming waves [42]. DEG-based WECs have non-linear response, therefore the conditions to maximise their energy transfer are non-trivial [43]. Nonetheless, it has been demonstrated [16, 17] that a resonant-like behaviour should still be pursued in order to enhance the power capture performance of the system.

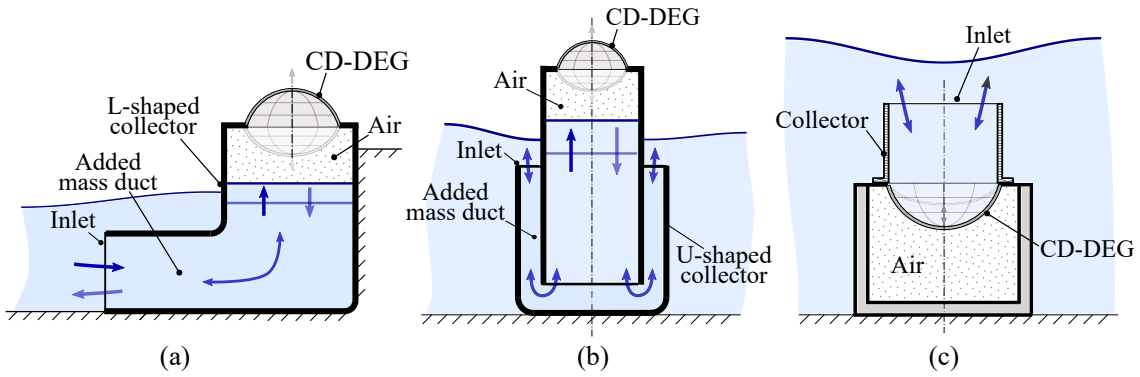

Figure 5: Advanced DEG-based WEC layouts with optimised dynamical response: L and U-shaped OWC collectors (a, b), DT-PD WEC with CD-DEG on top.

The design of resonant WECs with DEG PTOs requires tailored solutions aimed at counterbalancing the DEG stiffness either through a large hydrodynamic inertia or negative hydrostatic stiffness. In this regard, advanced OWC and PD solutions have been conceived.
As regards OWCs, it has been suggested that efficient coupling with the CD-DEG can be obtained using collectors in which the water column is connected to the open sea through a narrow channel (namely, an added-mass duct) that provides the system with increased added mass. OWC collectors featuring an L shape (Fig. 5a) [16] or a U shape (Fig. 5b) [17, 44] have been studied and tested experimentally in combination with CD-DEGs. L-shaped OWCs have a horizontal channel (parallel to the sea bed) as the added mass duct. U-shaped OWCs have a vertical added mass duct which can be implemented both as an axial-symmetric coaxial-duct [17, 45] or as a square-plan device [44, 46].
As regards PD WECs, a recently-patented [47] solution that enables the achievement of dynamical tuning with the waves is shown in Fig. 5c. The device, hereafter called the dynamically-tuned PD WEC (DT-PD WEC), has one (or several) CD-DEG(s) mounted horizontally on top of a submerged air chamber (either bottom-fixed or moored). The device optionally includes a vertical collector that channels the water flow towards the DEG. This layout realises a compensation of the CD-DEG elasticity through a negative hydrostatic stiffness contribution. In effect, a downward deformation of the CD-DEG corresponds to an increase of both the elastic restoring force of the DEG and the downward-pushing hydrostatic pressure from the surrounding water. The vertical duct acts as an added mass duct, thus increasing the hydrodynamic inertia of the WEC. Implementation of CD-DEG elasticity compensation allows the design of resonant DT-PD WECs over a wide range of device dimensions and predominant sea states.

3.4 Power electronics

In order for DEG PTOs to deliver the harvested energy to the electrical grid or to utilities, suitable power electronics is required. According to the operating cycle described in Sects. 2.1 and 3.1, such electronics should deal with the following requirements:

– Direct current (DC) high-voltage (HV) operation, required to implement electric fields in the order of $10^1 - 10^2$ kV/mm on DEGs.

– Bidirectional intermittent electrical power fluxes: electrical energy should be supplied to the DEG for priming (phase *P2* of the cycle in Sect. 2.1) and positively extracted during the following phases (*P3, P4*).

– Handling of larger currents (and powers) for short time intervals during priming and discharging phases (*P2, P4*), as opposed to lower currents during the rest of the cycle (*P3*).

The first point, which is often regarded as a limit in other DE applications, matches well with the electrical grid requirement. The second point requires the design of dedicated bidirectional DC-DC power converters. Finally, the third issue potentially leads to inefficiencies in the power electronics operation, unless a suitable balance is realised between the duration of the priming/discharging phase and the range of the operating currents. In [43], it has been shown that theoretical energetic performance is practically unaltered if the current absorbed/supplied by a CD-DEG PTO is limited and the duration of priming/discharging phases is $\sim 1/7$ of the whole cycle (instead of instantaneous).

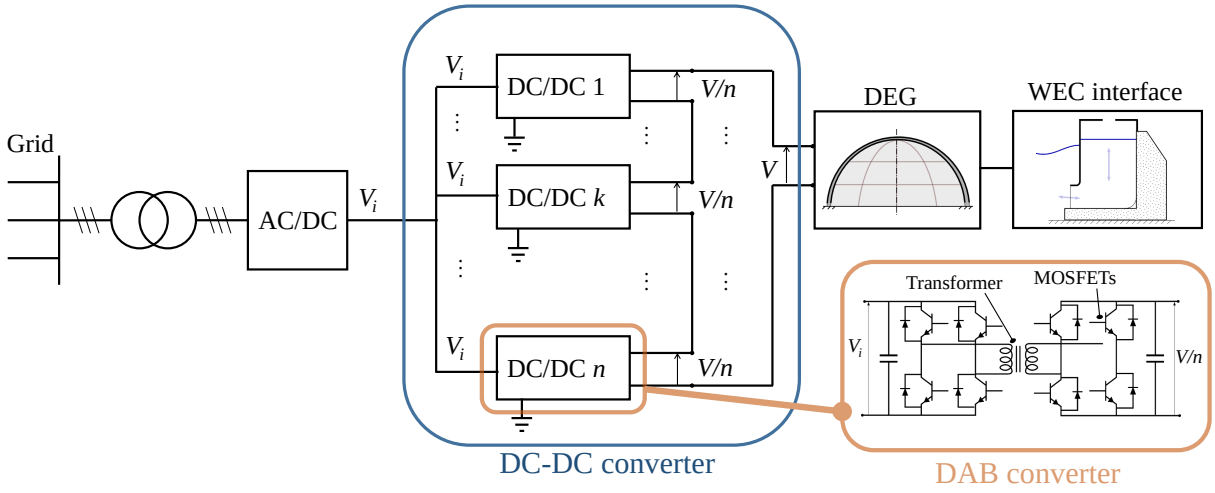

Figure 6: Example of the layout for grid connection and power electronics for a CD-DEG PTO. In this example, the DC-DC converter is realised by a cascade of modules in input-parallel output-series configuration. The inset shows the circuit schematic of a DAB module.

A schematic of a possible layout for grid connection of a WEC with a DEG PTO is shown in Fig. 6. The system includes: a bidirectional DC-DC converter, that is the DEG driver; a DC link that smooths the current absorbed/provided by the DC-DC converter; and an AC-DC converter (inverter) to feed the generated power to the grid.
The core element of the power electronics is the DC-DC converter. In the context of SBM Offshore's research on the S3 device, different DC-DC topologies have been proposed, namely dual-active bridge (DAB) [48] (see inset in Fig. 6) and flyback [25] converters. Both the configurations include a transformer to galvanically isolate the two sides of the DC-DC converter, and parallel-connected capacitors, on both sides of the bridge, to prevent overloads on the switching semiconductors. A fine tuning of the voltage profile on a DEG during each active phase of the operating cycle (*P2-P4*) can

be achieved by taking advantage of high-frequency switching of the semiconductors (tens/hundreds of kHz) and appropriate modulation strategies for the different phases.

Although the second solution features simpler architecture with less components, the DAB architecture is usually considered more suitable for high-power architectures [25].
To date, commercially available semiconductors compatible with the discussed specifications are practically unavailable. For this reason, it has been proposed [25, 48] that a possible implementation for the DC-DC electronics might comprise a cascade of modules (see Fig. 6). Such modular architecture is most often referred to as input-parallel output-series, and it consists of n DC-DC converters whose inputs are parallel-connected to the same bus voltage V_i (significantly lower than the total output voltage). The outputs of the converters are in series, so that each converter takes the n-th fraction of the total DEG output voltage V. DAB modules rated at 4 kW have already been built based on available components [48] and experimental tests showed efficiencies over 90 % during the characteristic charging/discharging transients of the DEG operating cycle.

4 Mathematical modelling

Numerical models are instrumental to carry out design-analysis, performance assessment, and evaluation of any WEC system. With reference to DEG-based WECs, owing to the complexity of nonlinear hydro-electro-elastic interactions, advanced numerical techniques are required to accurately model the physics of the problem, based, e.g., on the finite element method (FEM) or computational fluid dynamics. Unfortunately, those approaches are highly computationally expensive.
In this article, a general lumped-parameter modelling approach is proposed, valid for OWC and PD devices, which relies on some simplifications and enables faster-than-real-time simulations. Instead of providing an accurate and sophisticated description of DEG-based WEC response (which is not a priority at the present technological stage), this approach is intended as a tool for the design of new concepts. The model, which has been validated in [17], provides essential insight into the dynamics of DEG-WEC systems, allowing for the design of dynamically tuned devices.

4.1 Modelling approach

The proposed simplified modelling approach makes use of a global energy balance to derive the equations of motion of a DEG-WEC coupled system. It enables straightforward integration of WEC hydrodynamics and CD-DEG sub-models and makes it possible to consistently account for nonlinear contributions. This type of approach is widely employed in DE transducers modelling [26, 49]. Energy-based approaches have also been employed in hydrodynamic WEC modelling, leading to formulations consistent with the well-known Cummin's linear formulation [46, 50].
The study is restricted to consider OWC and PD WECs consisting of a fixed collector housing an oscillating fluid volume and mounting a set of identical CD-DEGs as the PTO.

For each WEC type, the model relies on the following assumptions:

- The system hydrodynamics are described by potential flow and linear wave theory.
- The CD-DEG is treated as a stretchable elastic ideal dielectric [26].
- The CD-DEG kinetic and gravitational potential energies are negligible compared to the elastic and electrostatic contributions, and to the water volume potential/kinetic energies (i.e., the DEG is assumed to operate in quasi-static conditions), as discussed in [43].
- For simplicity, hydrodynamic and elastic viscous energy losses and electrical DEG losses are neglected.

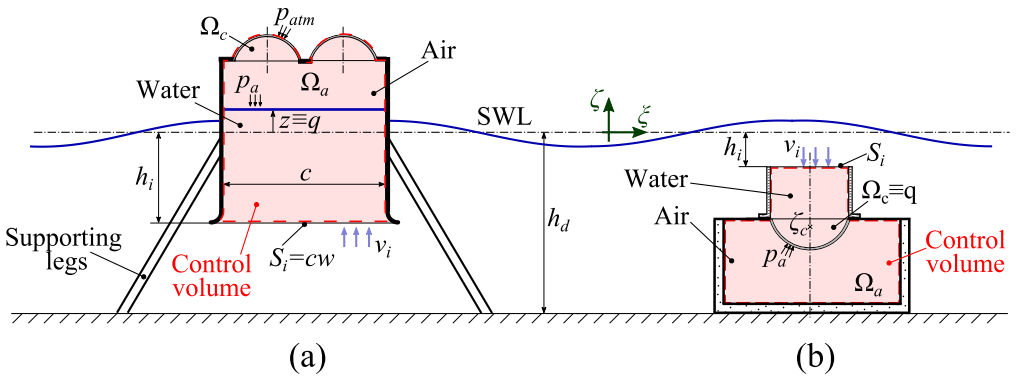

Figure 7: Control volume definition (shaded area) for (a) OWC and (b) PD WECs.

– A lumped-parameter approach is used and the system configuration is assumed to be uniquely described by a single degree of freedom, which identifies both the water volume and the DEG configuration. The system configuration is uniquely described by a generalised coordinate q.

A control volume is considered comprising: an oscillating water volume delimited by the collector walls and an inlet section (open to the sea); the DEG PTO; and closed air chambers possibly embedded within the WEC (see Fig. 7). For such a control volume, the following power balance holds:

$$\dot{\mathcal{E}}_k + \dot{\mathcal{E}}_g + \dot{\mathcal{E}}_a + \dot{\mathcal{E}}_m + \dot{\mathcal{E}}_e = \dot{\mathcal{W}}_i + \dot{\mathcal{W}}_e + \dot{\mathcal{W}}_{atm}. \tag{1}$$

where dotted quantities are differentiated with respect to time and the different terms have the meaning described in the following. $\mathcal{E}_k$ and $\mathcal{E}_g$ are the kinetic and gravitational potential energies associated with the water volume oscillation. $\mathcal{E}_a$ is the potential energy of the embedded air chamber. $\mathcal{E}_m$ and $\mathcal{E}_e$ are the elastic and electrostatic potential energies of the DEGs. $\dot{\mathcal{W}}_i$ accounts for the power supplied to the control volume by water flowing through the inlet section. $\dot{\mathcal{W}}_e$ is the electrical power supplied to the CD-DEGs by the power electronics. $\dot{\mathcal{W}}_{atm}$ is a term accounting for the work done by the atmospheric pressure on the CD-DEGs, in the case where they have a face in contact with the atmosphere.

The water volume kinetic energy has the following general form [51]:

$$\mathcal{E}_k = \frac{1}{2} M_q(q) \dot{q}^2, \tag{2}$$

where $M_q(q)$ is the generalised inertia of the water volume (generally depending on q).

The gravitational energy $\mathcal{E}_g$ of the water volume is also a function of the system geometrical configuration, namely $\mathcal{E}_g = \mathcal{E}_g(q)$.

Air pockets within the control volume are treated as ideal gas volumes undergoing adiabatic transformations, for which the following relation between the instantaneous air volume Ω_a and the absolute air pressure p_a holds:

$$p_a \Omega_a^\gamma = p_0 \Omega_0^\gamma, \tag{3}$$

where p_0 and Ω_0 are the pressure and volume in a reference configuration, and γ is the adiabatic index of air.

The internal energy $\mathcal{E}_a$ of the air volume reads as follows:

$$\mathcal{E}_a = p_a \Omega_a / (\gamma - 1). \tag{4}$$

Since Ω_a is solely a function of q, $\dot{\mathcal{E}}_a$ can be written as:

$$\dot{\mathcal{E}}_a = -p_0 \left(\frac{\Omega_0}{\Omega_a}\right)^{\gamma} \frac{\mathrm{d}\Omega_a}{\mathrm{d}q}\dot{q}. \tag{5}$$

Indicating with h_i the average depth of the inlet section of the collector, the power flowing through that section becomes:

$$\dot{\mathcal{W}}_i = S_i v_i \left(p_{atm} + \rho g h_i + p_w + e_g + e_k\right), \tag{6}$$

where S_i is the cross-sectional area of the inlet section, v_i is the flow velocity at that section, p_{atm} is the atmospheric pressure, ρ is the sea water density, g is the gravitational acceleration, p_w is a wave induced pressure (including the contribution from the incident, diffracted and radiated waves, as detailed in Sect. 4.2 and in [50]), and e_g and e_k are the mass gravitational energy density and kinetic energy density of the flow.
Choosing the still water level (SWL) as the zero-potential-energy set-point, $e_g = -\rho g h_i$ and it cancels out with the hydrostatic pressure contribution.
The velocity v_i can be expressed in the general form $v_i = \kappa_i(q)\dot{q}$, where κ_i results from a mass balance over the water volume (see the Appendix). The kinetic energy density e_k then reads as

$$e_k = \frac{1}{2}\rho v_i^2 = \frac{1}{2}\rho \kappa_i^2(q)\dot{q}^2. \tag{7}$$

With regards to the CD-DEGs, the elastic energy can be expressed solely as a function of the configuration, as clarified later in Sect. 4.3: $\mathcal{E}_m = N_D \mathcal{E}_{m,s}(q)$, where N_D is the number of identical CD-DEGs per WEC and $\mathcal{E}_{m,s}(q)$ is the elastic energy of a single CD-DEG. The electrostatic energy of the CD-DEGs is given by:

$$\mathcal{E}_e = \frac{N_D}{2} C V^2, \tag{8}$$

where $C = C(q) = Q/V$ is the capacitance of a single CD-DEG.
The power supplied to the DEG by the electronics is the product of the applied voltage and the supplied current, namely:

$$\dot{\mathcal{W}}_e = N_D V \dot{Q}. \tag{9}$$

The term $\dot{\mathcal{W}}_{atm}$ reads as follows:

$$\dot{\mathcal{W}}_{atm} = -\nu p_{atm} \frac{\mathrm{d}\Omega_c}{\mathrm{d}q}\dot{q}, \tag{10}$$

where Ω_c is the volume subtended by a single deformed CD-DEG cap (solely depending on q), and ν is the number of CD-DEGs having a face in contact with the atmosphere. In the OWC application, $\nu = N_D$, while in the PD application, $\nu = 0$.

Combining Eqs. (1-10) leads to the following general equation of motion for the system:

$$\begin{aligned} &M_q \ddot{q} + \frac{1}{2}\left(\frac{\mathrm{d}M_q}{\mathrm{d}q} - \rho S_i \kappa_i^3\right)\dot{q}^2 + \frac{\mathrm{d}\mathcal{E}_g}{\mathrm{d}q} - p_0 \left(\frac{\Omega_0}{\Omega_a}\right)^{\gamma} \frac{\mathrm{d}\Omega_a}{\mathrm{d}q} + N_D \frac{\mathrm{d}\mathcal{E}_{m,s}}{\mathrm{d}q} + \\ &- N_D \frac{V^2}{2}\frac{\mathrm{d}C}{\mathrm{d}q} + \left(\nu \frac{\mathrm{d}\Omega_c}{\mathrm{d}q} - S_i \kappa_i\right) p_{atm} = S_i \kappa_i p_w \end{aligned} \tag{11}$$

Besides non-linear air and CD-DEG contributions, it is worth noticing that the presented equation allows for the consideration of non-linear contributions in the hydrostatic and excitation forces, possibly due to the expressions of $\mathcal{E}_g$ and κ_i as functions of q. A further non-linear term, proportional

to $\dot{q}^2$, is also present and this is usually neglected in linear hydrodynamic WEC models [52].
Eq. (11) has to be combined with a set of complimentary equations to provide a closed-form formulation. Those include equations that relate M_q, $\mathcal{E}_g$, $\mathcal{E}_{m,s}$, C, Ω_a, Ω_c and κ_i to q. The calculation of those terms is detailed in the following subsections, whereas explicit application of Eq. (11) to the OWC and PD cases is discussed in the Appendix.
As regards the choice of coordinate q, in OWCs it is convenient to set q equal to the water column displacement. In PD WECs, q is conveniently taken equal to the CD-DEGs subtended volume, $q = \Omega_c$.

4.2 Hydrodynamic model

The contribution due to the wave field in the WEC dynamics is accounted for by the right-hand side term in Eq. (11). It is assumed that the wave pressure p_w can be modelled in accordance with linear wave theory [53]. As observed in [50], p_w is the sum of two terms: p_e, owing to the excitation wave pressure at the inlet section in a diffracted wave field, and p_r owing to wave radiation.
Treating real sea waves as a superposition of monochromatic waves with angular frequencies ω_i and crest-to-trough heights H_i (generated according to a spectral distribution), p_e can be expressed in the following general form

$$p_e = \sum_i \frac{H_i}{2} \gamma(\omega_i) \cos(\omega_i t + \varphi_i), \tag{12}$$

where t is time, φ_i are random phases and $\gamma(\omega)$ is a frequency-dependent excitation coefficient.
The radiation contribution can be expressed in the following general form [50, 52]:

$$p_r = -m_\infty \ddot{q} - \int_0^t k_r(t-\tau)\dot{q}(\tau)\mathrm{d}\tau, \tag{13}$$

where m_∞ is a coefficient representing the contribution of the infinite frequency added mass (which adds on to the control fluid volume inertia, M_q, in Eq. (11)) and k_r is called the retardation function. The calculation of $\gamma(\omega)$, m_∞ and the frequency transform of $k_r(\tau)$ can be performed using well-established frequency-domain radiation/diffraction codes implementing the boundary element method (BEM) [54]. Such a method makes it possible to calculate the above-mentioned parameters in a linear fashion and in correspondence to a reference equilibrium configuration. In particular, some BEM solvers [55] include a facility to model bodies whose motion is described by generalised kinematic coordinates (instead of the standard 6 rigid-body modes of motion), as in the case of PD WEC modelling.

The other hydrodynamic parameters, M_q, $\mathcal{E}_g$, κ_i, can be calculated based on geometrical considerations (see the applications in the Appendix). Alternatively, by including the control fluid volume within the BEM simulation, linearised expressions for M_q and $\mathrm{d}\mathcal{E}_g/\mathrm{d}q$ (calculated in a reference equilibrium position) can be obtained.

4.3 CD-DEG model

In order to compute the CD-DEG elastic energy, $\mathcal{E}_{m,s}$, and capacitance, C, lumped parameter models are considered. In particular, the CD-DEG deformation kinematics is approximated by a single degree of freedom (instead of a continuum model), as suggested in [15]. This hypothesis has the following implications: 1) the set of the possible CD-DEG shapes in the presence of electrical activation is the same as in the absence of activation (though the CD-DEG configuration is assumed to change as a result of voltage application); 2) in the case where the CD-DEG directly contacts sea

water, the set of deformed shapes in dynamical operating conditions is the same as that provided by the static DEG response.

Lumped-parameter CD-DEG modelling has been discussed in [15,17], introducing the following assumptions:

- The DE is a lossless hyperelastic material [26].
- The deformed CD-DEG has the shape of a spherical cap, whose geometry is entirely described either by the tip displacement h (see Fig. 3) or by the subtended volume Ω_c.
- The stretch is variable throughout the CD-DEG but it is everywhere equi-biaxial (i.e., meridian and circumferential stretches are equal).
- Electrically, the CD-DEG is a stack of thin parallel-plate capacitors with non-uniform thickness.

Owing to the first hypothesis, Ω_c and h are related as follows:

$$\Omega_c = \frac{\pi}{6} h(h^2 + 3e^2). \tag{14}$$

Owing to the equi-biaxial stretch assumption, the stretch distribution in a configuration identified by h is [15]:

$$\lambda = e e_0 \frac{h^2 + e^2}{e^2 e_0^2 + h^2 R^2}. \tag{15}$$

where R is the distance of a generic material point from the axis in the unstretched configuration (see Fig. 3a). Since the DE is a hyperelastic material, the elastic energy is expressed through the strain-energy function [26], Ψ, as:

$$\mathcal{E}_{m,s} = \int_0^{e_0} 2\pi t_0 R \Psi(\lambda) \mathrm{d}R. \tag{16}$$

The relationship $\Psi(\lambda)$ is then expressed by means of an appropriate constitutive hyperelastic model [56]. The simplest hyperelastic model is Neo-Hookean model, according to which Ψ depends on the stretch λ and shear modulus μ as follows:

$$\Psi(\lambda) = \frac{\mu}{2} \left(2\lambda^2 - \lambda^{-4} - 3\right). \tag{17}$$

Assuming that the thickness of the electrodes is negligible compared to that of the dielectric, the CD-DEG capacitance is given by the following equation:

$$C = \frac{\pi \varepsilon n_L^2 \lambda_p^2 e^2}{3 t_0} \left[\left(\frac{h^2 + e^2}{e^2} \right)^3 + \left(\frac{h^2 + e^2}{e^2} \right)^2 + \frac{h^2 + e^2}{e^2} \right], \tag{18}$$

where n_L is the number of layers in the DEG stack.

In [15], it has been demonstrated that the presented equations provide good agreement with FEM results over a wide deformation range and in cases where the CD-DEG faces are subjected to a uniform pressure difference. In cases where the CD-DEG is subjected to a pressure distribution which depends on its deformation (as in the PD WEC application), an alternative approach is to perform a static FEM analysis of the DEG response (for instance, in the DT-PD WEC case, by investigating the CD-DEG deformed shape at different values of the overlying water head) and then map the values of $\mathcal{E}_{m,s}$ and C accordingly.

As $\mathcal{E}_{m,s}$ and C uniquely depend on Ω_c (or h), their derivatives with respect to q (used in Eq. (11)) can be calculated by the chain rule, since Ω_c (or h) is only function of q, as postulated in Sect. 4.1.

The instantaneous value of the voltage V on the CD-DEG depends on the control strategy. The net amount of electrical power generated by the CD-DEG (either stored in the DEG electric field or supplied to the power electronics) is given by:

$$\frac{1}{N_D}\left(\dot{\mathcal{E}}_e - \dot{\mathcal{W}}_e\right) = -\frac{V^2}{2}\dot{C} \tag{19}$$

and this shows that electrical energy is positively generated while the CD-DEG capacitance is decreasing ($\dot{C} < 0$), which is consistent with the operating cycle description provided in Sect. 2.1.

5 Experimental deployment of WECs with DEG PTO: an overview

This section presents an overview of prototype demonstrations of CD-DEGs and integrated WECs equipped with DEG PTOs. Compared to other PTO systems, DEGs' control and electrical functionalities include the capability of generating electrical power output from the input mechanical energy source even at a reduced scale. Based on that, a wide set of experimental models have been developed, starting from small-scale laboratory test-benches and progressively obtaining the target of electricity generation from wave tank waves up to a scale of 1:30. The prototypes reviewed here represent the first attempts to lead DEG technology beyond the Watt power scale. The first part of this section illustrates some novel/dedicated scaling rules that enable testing of coupled DEG-WEC systems in conditions of hydrodynamic similarity. Then, a short survey on experimental activities concerned with the application of CD-DEG PTO systems is presented.

5.1 CD-DEG PTO scaling

In order to reproduce the full-scale dynamics of a marine energy device in small-scale experiments, testing in hydrodynamic similarity conditions is required. In the case of WECs, the criterion of Froude scaling applies [57]. Froude scaling provides a series of scaling coefficients (which are powers of the WEC geometrical scale factor, s_f) for the different physical variables involved in the experiment. Owing to the peculiar electro-mechanical response of DEGs, uniformly scaling the dimensions of a CD-DEG by the scale factor does not provide a DEG response consistent with the Froude scaling rules. Nonetheless, consistent scaling can be achieved by applying different scale factors to the different DEG dimensions [17].

It should be initially observed that, according to Froude rules, the pressure difference between the CD-DEG faces should scale proportionally with s_f [57]. For simplicity, it is assumed that the CD-DEG faces are subjected to a uniform pressure difference p (similar considerations can be drawn in the case when a non-uniform pressure distribution acts across the CD-DEG). In that case, the following energy balance on the CD-DEG holds (see Sect. 4.1):

$$N_D p\dot{\Omega}_c + \dot{\mathcal{W}}_e = \dot{\mathcal{E}}_m + \dot{\mathcal{E}}_e, \tag{20}$$

Substituting Eqs. (8-9) into the previous balance then leads to the equation for p below:

$$p = \frac{\mathrm{d}\mathcal{E}_{m,s}}{\mathrm{d}\Omega_c} - \frac{V^2}{2}\frac{\mathrm{d}C}{\mathrm{d}\Omega_c}. \tag{21}$$

The voltage V further relates to the electric field distribution over the CD-DEG, which reads as follows:

$$E = n_L \lambda^2 V / t_0. \tag{22}$$

It is assumed that, at the different testing scales, the employed DE materials have the same or similar constitutive properties (in terms of the hyperelastic and dielectric parameters). Moreover, the applied voltage is scaled in such a way that the electric field E (Eq. (22)) is the same at different scales (regardless of the number of layers). It is also assumed that the DEG radial dimensions (e and e_0) scale with s_f. With this assumption, if the CD-DEG displacements (e.g., h) scale with s_f, the stretch λ and the strain-energy density Ψ are scale-invariant.
Based on Eq. (21), in order for p to scale with s_f, the CD-DEG thickness, t_0, (to which $\mathcal{E}_{m,s}$ and C are proportional) should scale with s_f^2 (instead of the geometric scale factor, s_f). In practice, the CD-DEG thickness dramatically decreases as the scale of the experiment is reduced.

In the presence of embedded air chambers within the WEC prototype, dedicated scaling rules should also be applied to properly scale the rigidity associated with the air compressibility [58]. For example, in small-scale devices, embedded air chambers should be enlarged through the use of external reservoirs, as suggested in [59]. However, this solution introduces technical complexity, energy losses and possible non-uniformity in the air pressure. For those reasons, in the experiments on DEG-based OWCs described herein, air chamber scaling has not been pursued. As a consequence, the device dynamics at larger scales would be slightly modified due to the the larger air chamber compressibility.

5.2 Review of CD-DEG PTO prototypes testing

This section presents a survey of the results of experimental campaigns carried out on CD-DEG PTO systems for wave energy application.
Three classes of experiments are considered:

- Functional dry-run experiments on the CD-DEG topology.
- Wave-tank testing of a set of OWCs with CD-DEG PTOs. The tested prototypes are the result of improvements, addressed through the years, aimed at enhancing dynamical tuning and providing scalable architectures, suitable for future full-scale deployment.
- In-field tests on a scaled OWC with CD-DEGs, installed in a benign sea test site. Those tests were aimed at assessing the dynamical response and survivability of the system in real sea conditions.

An overview of the experimental results is provided in Table 2. In particular, the table shows the features of the experimental CD-DEG prototypes and (when present) the OWC collectors, and the sea state testing conditions (either regular or irregular waves). For tests in which electrical DEG functionality was implemented, the range of the applied electric field and the device power output (in the test and projected to full-scale) are reported. Full-scale equivalent power is obtained by multiplying the prototype power by the scale factor to the power of 3.5, as per the Froude criterion [57]. For constant-frequency tests (namely, regular wave tests), the steady-state converted energy density is also shown.

The tests reviewed in Table 2 were carried out using VHB 4905 acrylic (by 3M) as the DE material and painted carbon-grease electrodes. This material is widely used as the DE in demonstrators, due to its low rigidity and ease of handling. For example, using VHB films pre-stretched by $\lambda_p > 3$ allows the implementation of thin CD-DEGs (as required by the scaling rules in Sect. 5.1) while suppressing the need for extremely thin (commercially unavailable) unstretched membranes.

Similar to previous experimental works on DEGs [6], the control of the CD-DEG prototypes was implemented through simplified circuits [16, 17, 32] that are suitable for the measurement and control of the generation cycle described in Sect. 2.1 at laboratory scale, even if this does not allow

the actual output and storage of the generated energy. In particular, the charging phase *P2* was performed by connecting the DEG to a power supply. During the generation phase *P3*, the DEG was connected in-parallel to a buffer capacitor, in which the charge was transferred. Discharging phase *P4* was implemented by draining the charge on DEG to ground through a resistor. The net power generated by the DEGs (regardless of losses in the control circuit) has been estimated accordingly, based on the measured voltage on the CD-DEG and on the buffer capacitor.
The maximum electric field used in the tests was in the range 100-200 kV/mm which is compatible with the dielectric strength of VHB that improves with stretch, in a similar way to other rubber-like dielectrics [7]. The maximum energy density (per unit DE mass per cycle) achieved in the presented experiments was in the order of 0.2 kJ/kg. This value is roughly 1/4 of the maximum experimental performance reported in literature for the same acrylic DE [6], achieved using an equibiaxial stretcher, which allows a better/uniform exploitation of the material but is rather impractical for real world WEC applications.

The material employed in the tests featured large dielectric and viscoelastic losses (see Table 1) and is considered unsuitable for larger-scale installations. Despite this, the results presented herein provide a significant measure and a lower bound of the performance of the investigated concepts. Existing silicone DE materials already exceed the dielectric properties of acrylic, and they might play a crucial role towards future upscaling stages, while leading to an improvement in performance [29].

Table 2: Overview of dry-run, wave-tank, and in-field tests specifications and results.

			Wave-tank tests				Sea-tests
		Dry-run tests	Square-base OWC	L-shaped OWC	Floating tubular OWC	U-shaped axial-sym OWC	U-shaped square-base OWC
	scale	1:70/60	1:50	1:40	1:50	1:30	1:8
CD-DEG features	N_D	1	1	1	1	1	3-4
	e (mm)	65	90	125	97.5	195	195
	t_0 (mm)	1.5	1	1.5	1	2-3	4-5
	λ_p	3.5	3.6	4	3.7	3.5	3.4
	n_L	1	1	1	1	2	N/A
	E (kV/mm)[1]	45-120	25-50	40-180	55-190	45-100	N/A
OWC dimensions	breadth/diam. (mm)	N/A	260	970	200	600	1.5
	width (mm)	N/A	285	370	200	600	3.79
	water depth (m)	N/A	0.2	0.35	2	2	1.7
Regular wave tests	Wave height H (mm)	15-45	20-40	30-90	75-100	100-250	N/A
	Wave freq. f (Hz)	0.6-1.2	0.6-1.3	0.5-1.1	0.3-1.0	0.3-0.7	N/A
	Power output (W)[2]	0.15	0.08	0.9	0.06	3.8	N/A
	Full-scale equiv. power (kW)	250-430	68	360	53	560	N/A
	Energy density (kJ/kg)[3]	0.05	0.03	0.14	0.05	0.19	N/A
Irregular wave tests	Signif. wave height H_s (mm)	N/A	N/A	N/A	75-150	125-175	150-450
	Peak freq. f_p (Hz)	N/A	N/A	N/A	0.45-0.63	0.4-0.6	0.3-0.55
	Power output (W)[2]	N/A	N/A	N/A	0.02	1.0	N/A
	Full-scale equiv. power (kW)	N/A	N/A	N/A	18	150	N/A

[1]Maximum electric field on the CD-DEG in different tests
[2] Average power output in the best sea state
[3] Average energy density in the best sea state

5.2.1 Dry-run tests

Dry-run laboratory experiments enable 1) the verification of the PTO system response compared to predictive models; 2) the assessment of the PTO performance in terms of efficiency and convertible power; and 3) the implementation of control algorithms.
To test CD-DEG PTOs, a custom test-bench was built [60], which recreates the operating conditions of an OWC air chamber with a DEG PTO on top of it. This device is capable of mounting small-scale CD-DEGs (up to 130 mm diameter) and is equipped with conditioning and control electronics. The setup comprises a mechanical sub-system consisting of a cylindrical air chamber and a rigid piston (emulating the water column) driven by a linear motor. The system is fully-sensorised, thus allowing the measurement of the piston position, the air chamber pressure and the CD-DEG tip displacement. A picture of the setup is shown in Fig. 8a.
The setup has been employed for different types of tests, including electrical power generation tests with prescribed DEG deformation [60], and hardware-in-the-loop (HIL) tests, in which a numerical dynamic WEC model is used to drive the piston motion [61]. Besides tests with acrylic CD-DEGs, tests on samples with silicone-based dielectric and electrodes have been recently performed, showing improved conversion efficiency and converted energy density of up to 0.15 kJ/kg [32].

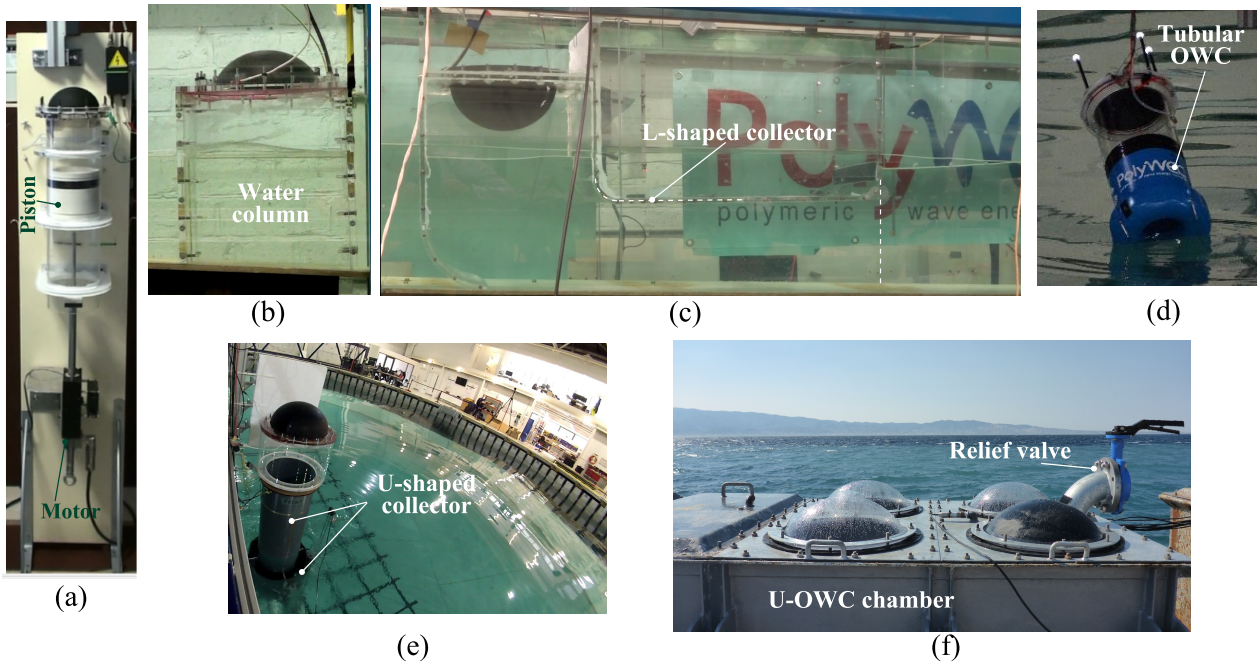

Figure 8: Pictures of the the different experimental prototypes. (a) Dry-run test bench for CD-DEGs. (b) Square-base OWC. (c) L-shaped OWC. (d) Floating tubular OWC. (e) U-shaped axial symmetric OWC. (f) Sea-tests on square-base U-shaped OWC.

5.2.2 Wave-tank tests

It is widely recognised that wave-tank testing is a necessary step towards the development of new marine energy devices [57]. In effect, tank tests on WEC prototypes provide insights into the device response and benchmark data for the validation/refinement of models, while requiring reduced operational effort compared to in-field tests.

In the framework of the research activities reviewed in this paper, several wave-tank tests on

OWC prototypes with CD-DEGs have been performed. First, two small-scale prototypes (up to 1:50 and 1:40) of bottom-fixed OWCs were tested in regular waves in the wave flume facility at Edinburgh University [62]. In those experiments, the prototypes had a width equal to that of the wave tank, and radiated and diffracted waves generated by the device, as well as the undisturbed incident waves, propagated in a single direction (namely, the flume longitudinal direction). Following this, two OWC prototypes with an axial-symmetric shape were tested at the FloWave test tank [63] in Edinburgh University: a small floating OWC (with scale of 1:50) and a larger prototype featuring an axisymmetric U-shaped collector (scale 1:30) [17]. Both prototypes were tested in regular and irregular waves.
The outcomes of those tests can be summarised as follows:

- The operating principle of the devices was demonstrated; indeed, electrical power generation from wave power was successfully achieved in all of the tests.
- Design procedures for dynamically tuned devices (resonating at a target wave frequency) were demonstrated and numerical models were validated.
- Some of the tested samples are among the largest and most powerful DEGs built to date, and they represent a major step forward towards scaling-up and manufacturing of large-scale DEGs.

The first DEG-based OWC prototype consisted of a square-based OWC collector (similar to that schematically depicted in Fig. 1c) and a CD-DEG as the PTO. A picture of the device is shown in Fig. 8b. That prototype was designed with the aim of proving the concept of a DEG-OWC for the first time. Therefore, at that stage, attention was not addressed to the optimization of device dynamical response. As a consequence, the device showed modest energy capture performance, with maximum power output in the order of a few tens of milliwatts (see Table 2) [40].
With the aim of improving the dynamic performance, a second prototype was developed (Fig. 8c) based on an L-shaped OWC collector (as described in Sect. 3.3 and Fig. 5). The horizontal added mass duct was designed in such a way as to set the device's natural frequency within the testing wave frequency range. The device mounted a CD-DEG with radius $e = 125$ mm and pre-stretched thickness $t_p = 94$ μm, corresponding to $e = 5$ m and $t_p = 0.15$ m at a scale 40 times larger than of the prototype size (according to the scaling rules described in Sect. 5.1). The device delivered maximum power output of 0.9 W (corresponding to more than 350 kW at full-scale) in the presence of waves with frequency $f = 0.7$ Hz (corresponding to the device natural frequency) and height $H = 90$ mm, corresponding to full-scale waves with $f = 0.11$ Hz and $H = 3.6$ m. Despite large dissipations in the acrylic material, wave-to-wire efficiencies of up to 20% were achieved. An extensive description of the prototype design and testing is provided in [16].

The above prototype concepts have a limited potential for full-scale application. In effect, they are representative of shore-based OWCs integrated in shallow water marine structures, but they are not suitable for offshore installations, which are the most promising for large wave farm deployments. With the aim of better representing potential full-scale architectures, two axial-symmetric DEG-based OWC prototypes were deployed and tested. In contrast with the previous experiments, the prototypes were tested both in regular and irregular waves to assess their potential performance in operating conditions closer to the real ones.
The first axial-symmetric prototype was based on an existing OWC concept proposed by the Spanish company Sendekia [39] and it had a floating tubular-shaped collector with a bottom aperture with a convergent-divergent shape (similar to the concept shown in Fig. 4a). The device, shown in Fig. 8d, was fixed to the tank bottom by means of tension leg moorings. It generated an electrical

power output of up to a few tens of milliwatts, corresponding to a few tens of kilowatts at a full-scale of 50:1. Such a reduced power output (compared to that of previous experimental tests) is due to two reasons: 1) hydrodynamic dissipations originated by the collector heave and surge oscillations; 2) lack of dynamical tuning with the incoming waves. In particular, the prototype was built by retrofitting an existing OWC collector with a CD-DEG, without consideration of the resulting dynamics that was, indeed, non-resonating. Despite sub-optimal performance, tests on that prototype provided evidence of the effectiveness of prediction-free control strategies for DEG PTOs (like those described in Sect. 2.1) in both regular and irregular waves.

The last and most advanced prototype featured the axisymmetric U-OWC architecture discussed in Sect. 3.3 and shown in Fig. 5b. The device is based on a U-shaped collector with an outer added mass duct of 600 mm in diameter and an internal water column of 400 mm in diameter. In the experiments, the collector was fixed to the tank bottom through a rigid structure (though in practice this device can also be implemented as a floating WEC). In contrast with the previous tests, the employed CD-DEG prototypes had multi-layered architecture, with two in-parallel DE layers. The PTO radius was $e = 195$ mm and its pre-stretched thickness t_p was in the range of $0.16 - 0.24$ mm (different thicknesses were used in different tests), corresponding to $e = 5.85$ m and $t_p = 0.155 - 0.22$ m at full scale (roughly, 30 times the prototype scale). A picture of the device is shown in Fig. 8e. Similarly to the previously discussed L-shaped OWC prototype, the collector was designed so as to set the resonance frequency of the coupled DEG-WEC system within the testing wave frequency range. A complete description of the results from the testing campaign is presented in [17]. Examples of experimental power curves in a set of regular and irregular waves are shown in Fig. 9 (solid lines). At different wave heights, the power output is maximum in a range of frequencies (peak frequencies, in case of panchromatic tests) between 0.5 and 0.6 Hz, in correspondence to the device's resonant frequency. The prototype generated maximum steady-state power output in the order of 1-4 W (150-600 kW full-scale equivalent), which is among the largest power outputs demonstrated to date with DEG prototypes.

The experimental data from this campaign were used to carry out an extensive validation of the modelling approach discussed in Sect. 4.1. In [17], it was demonstrated that the model efficiently predicts the device natural frequency and separately captures nonlinear effects due to the DEG and the hydrodynamics. In Fig. 9, the measured electrical power output (solid lines) is compared with the experimental predictions (dashed lines) for both the cases with regular and irregular waves. The model overestimates the value of the generated power by up to 30 % of the measured value. This is due to the electrical losses (in the acrylic DE and the electrodes), that are not taken into account, and the simplified rate-independent model used for the capacitance variation prediction (see Eq. (18)). In contrast, in [17] it is shown that the numerical trends of the dynamic variables (water column level, CD-DEG tip displacement, air pressure) are predicted with much better accuracy. Despite this, the model clearly captures the main features of the system dynamical response, namely:

- The oscillation amplitudes of the state variable and the power output are maximum at a frequency of ~ 0.55 Hz at any wave height.
- Although the incident wave power increases with the square of the wave height, the device power output has a lower increase rate (see Fig. 9a) owing to a progressive saturation in the CD-DEG deformation.

Overall, the model validation discussed in [17] widely confirms that the presented modelling approach is a valid tool for the design of dynamically tuned WECs with CD-DEG PTOs.

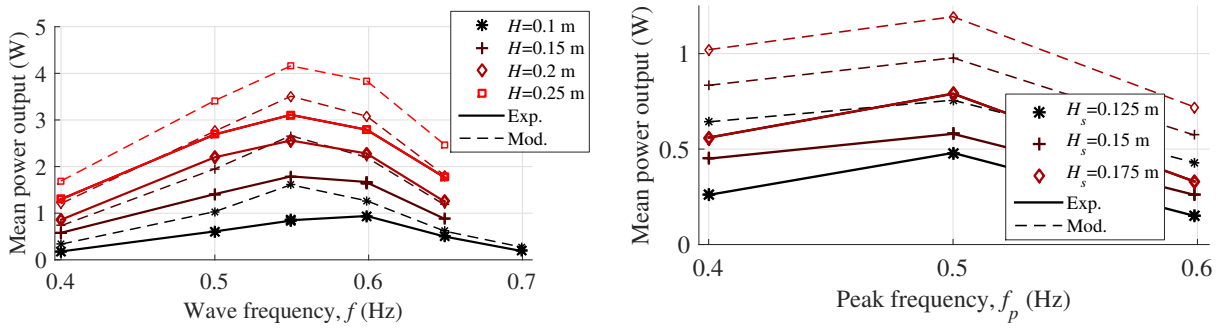

Figure 9: Average electrical power output (experiments and model) of a prototype of U-OWC with CD-DEG PTO (see Fig. 8e) in different sea states. (a) Regular wave experiments, (b) Irregular wave experiments.

5.2.3 In-field tests

Compared to wave-tank tests, sea trials on new WEC concepts provide insights into: 1) installation and operation procedures at sea; and 2) device continuous operation in real waves and severe sea conditions.

A first set of sea trials on an OWC with a CD-DEG PTO was recently carried out in the Mediterranean Sea, in the benign sea test site of the Natural Ocean Engineering Laboratory (NOEL) in Reggio Calabria, Italy [44]. The sea states typically recorded at NOEL consist of pure wind waves representing open-sea waves at a scale of approximately 1:10-1:8 in Froude similarity conditions [64]. Tests with a CD-DEG PTO were carried out by retrofitting a 1:8 scale model of a U-OWC available at NOEL, originally designed to resonate within the range of incident wave frequencies at the test site [50]. The U-OWC prototype consists of a square-based caisson integrated into a breakwater and equipped with an additional vertical channel that connects the water column to the open wave field, as discussed in Sect. 3.3. In contrast with the previous wave-tank tests, in which the OWC prototypes had a single CD-DEG with equivalent full-scale diameter in the order of 10 m, in these tests the PTO was split into several CD-DEGs, each with a diameter of 390 mm (approximately 3 m at full scale). In view of a full-scale installation, this solution allows easier DEG manufacturing and better robustness with respect to DEG faults. In the experiments, the CD-DEGs were studied only from a mechanical point of view, without implementing their electrical activation. A picture of the U-OWC with four DEGs is shown in Fig. 8f and an overview of the experimental results is provided in [44].

The main outcomes of the experimental campaign can be summarised as follows:

- The design procedure for the PTO was validated. In particular, it was observed that, although the CD-DEGs cause a modification in the natural frequency of the OWC, the natural frequency of the device still remains within the range of the typical incident waves.

- It was observed that a relief valve can be efficiently employed as a security measure to limit the CD-DEGs deformations in the presence of rough sea conditions, and as a measure to compensate for drift in the air chamber pressurization due to slight modifications in the tidal level at the test site.

6 Discussion on challenges, opportunities and roadmap

To date, DE transducers have been mainly used as sensors and actuators for low-power small-scale applications, and related commercial products are confined to pressure valves for automotive industry, stretch sensors, and low power energy harvesters from human motion [65]. As discussed in the previous sections, recent advances in the field of DEGs for wave energy has led to the development of small-scale prototypes (up to a few Watts of nominal rated power). Despite the good performance demonstrated in the experiments and the potential for future improvement, the success of DEG in the marine energy sector ultimately depends on their ability to enable electricity generation from wave energy at a competitive price. To achieve this goal, several open issues need to be addressed in the near future in order to bring DEG technology into operation at large-scale and in real scenarios. This section briefly outlines the status of DEG-PTO technology through techno-economic considerations, discusses the main challenges to overcome and outlines the opportunities that could be opened up by further research efforts.

6.1 Techno-economic considerations

Despite the promising features in terms of performance and architectural simplicity, the penetration of DEG into the energy market will depend on their actual ability to provide a step change in terms of technical and economic indicators. The success of a marine energy technology ultimately depends on its economic sustainability, quantified through the levelised cost of energy (LCOE) [66,67]. Such an indicator draws a synthesis of the combined contribution of different parameters, including energy yield, DEGs lifetime and component/operation costs.

Compared to most technologies employed in the wave energy sector, DEGs currently feature a rather low level of technological maturity, as their application is currently limited to small-scale prototype demonstrations. As a consequence, a high level of uncertainty affects most of the sensitive parameters influencing the techno-economic performance. This makes it difficult to formulate an accurate estimate of their LCOE. However, some general considerations have started to be drawn and preliminary LCOE assessments can be complemented by sensitivity analyses over uncertain parameters. This allows the identification of target values for such currently uncertain parameters required to make the DEG-PTO economically viable. In the past, the LCOE metric and methodology has been applied to some of the DEG-based WEC concepts described in the present paper. For instance, in [68], the techno-economic performance of the OWC plant on the Pico Island in Azores (Portugal) was assessed, with two PTO alternatives being considered and compared: an air turbine and a CD-DEG.

With reference to a hypothetical installation scenario for a WEC, the main parameters affecting the LCOE can be sorted into: capital expenditures (CAPEX), operational and decommissioning expenditures (OPEX), and annual energy production (AEP). The first two categories measure the costs involved the construction and operation of an ocean wave farm, while AEP is the estimate of the energetic performance.

The impact of a DEG PTO on a farm CAPEX depends on the achievable cost for a DEG in a market-scale perspective after industrialisation. Such a cost can be further split into material and manufacturing costs. Materials available on the market for DE application currently have prices between 50 €/kg (raw material) and 1000 €/kg (high quality dielectric films) to the general public. Such prices clearly are the result of low production volumes and extremely limited market share of DE products, and, in the case of dielectric films, they are almost entirely due to manufacturing costs. Looking at the current price of raw polymeric materials (e.g., the cost of natural rubber is in the range of few Euros per kilogram), it appears quite reasonable that the potential for price reduction

upon industrialisation and mass production could be very large. An ambitious but plausible target in the perspective of a large-scale economy for DEG PTOs, is to obtain a dramatic reduction in manufacturing process costs, down to the same order of magnitude of the material costs, with the latter progressively approaching that of commonly used elastomeric raw materials. In this regards, the development of DEGs is also expected to benefit from learning effects, as it has been observed in other electricity supply technologies such as solar photovoltaic or wind [69, 70]. Reduction in DEG PTOs cost would be driven by learning-by-doing (e.g. optimization of the manufacturing process), learning-by-researching (e.g. implementation of design innovations) and economies of volume (i.e. mass production) and scale (i.e. upscaling of the device rated power). Nevertheless, even if such a dramatic reduction of the DEG PTO cost is achieved, the economic viability of a potential WEC concept might be hindered by large infrastructural costs (collectors, mooring and foundations), which might greatly surpass the PTO cost. If this was the case, a transition should be sought towards fully-compliant device, in which the share of structural parts is minimised and lightweight fully-polymeric solutions are pursued (see discussion in Sect. 6.3).

As regards OPEX, the main unknown performance indicator is the long-term behavior of DEG PTOs and, hence, the cost for required replacements/maintenance over the lifetime of the wave energy plant. The achievable cyclic lifetime of DEGs strongly depends, in turn, on the manufacturing processes employed at industrial scale. In principle, a low-cost DEG PTO would make multiple replacements over the project lifetime affordable. This possibility is however strongly dependent on the required operational costs for replacement and decommissioning of the PTO systems. The traditionally high costs of marine operations indicate that, in a scenario of large offshore wave farms, highly reliable DEG PTOs would be required, while nearshore installations allow greater room for multiple replacements over the project life.

As regards the AEP, predictive models used for design provide a reasonable estimation of the producible energy, and improved estimations can be obtained by combining advanced numerical models and experimental data. Related uncertainties regard the expected efficiency of a DEG PTO at large scale. In effect, although established scaling laws (Sect. 5.1) enable consistent scale-up of experimental results in terms of the dynamic response, they are not accurate in upscaling loss effects (namely DE viscosity and dielectric losses) that compromise the efficiency. Further uncertainty relates to availability, in the form of the shutdowns required for DEG maintenance and replacement, and the associated losses in the energy yield.

6.2 Technological challenges

Upscaling of DEGs for wave energy application represents a complex challenge that involves a diversity of engineering fields, including material science, manufacturing and electronic engineering. Current technological challenges towards the large-scale applications can be divided into *performance* and *manufacturing challenges*.

Regarding *performance challenges*, experimental tests reviewed in Sect. 5.2 showed that DEGs can convert large energy densities (in the order of 0.1-0.2 kJ/kg) in dynamic operating conditions coupled to WECs. The main challenge thus relates to uncertainties on the long-term cyclical operation. The duration of a DEG depends on the number of mechanical and electrical loading cycles that the device and materials are able to withstand during their useful life. To date, available data mainly regards mechanical fatigue lifetime of rubber-like materials, both in dry-run and wet-run conditions [71, 72]. According to those studies, rubber samples operating in the stretch range of DEGs might last tens to hundreds of millions of cycles exceeding the target of 20 years for a WEC lifetime. On the other hand, little knowledge is available on the log-term performance of DEGs subject to cyclic electrical loading. Some studies on DE actuators claim a lifetime of at

least 5-10 million cycles, with little observable performance degradation [73, 74]. However, the seminal work [75] demonstrated that the large electric fields typically required to obtain large convertible energy densities are likely to reduce the devices' lifetime. In the context of the research on DEGs for WECs, a systematic study of the electrical fatigue lifetime of DE samples has been recently initiated [76]. Statistical models of DE breakdown upon cyclic electrical activation have been derived, and set-ups to test batches of DE samples have been built. Ongoing activities thus include the cyclic lifetime characterisation of improved DE samples, based on high-quality silicone films, with electrodes manufactured according to reliable procedures. Preliminary results on the silicone elastomers have highlighted that lifetime in the order of millions of cycles can be reasonably expected when high-quality DE films are considered [77].

Regarding *manufacturing challenges*, the implementation of large-scale DEGs (in the range of 100-500kW) for WECs requires the industrial production of large membranes (5-10 m in diameter) that are made from highly deformable materials (with elongation of up to 200-300%). These membranes must have a multilayer structure in which conductive layers are alternately bonded with dielectric layers. Additionally, the external faces of the membrane-assembly could be covered by a passive watertight elastomeric layer that acts as a barrier against water seepage.
Industrial production of single-layer DE membranes is to date pursued up to a limited scale (A4 sheets and rolls with a width up to 1.4 m). These solutions can already be employed for the implementation of intermediate scale prototypes for research purposes. Continuous production of rubber and silicone sheets is achieved through established industrial processes. Calendering production lines, dealing with the automatic mixing of compounded materials and shape setting through a cascade of rolls [78, 79], are all largely established in the plastic industry. Such processes offer the opportunity for a straightforward increase in the size of commercial elastomeric sheets.
As regards DE transducer assembly manufacturing, a number of researchers are currently focusing their efforts on the identification of scalable processes for the fabrication and bonding of compliant electrodes on DE silicone layers. Processes under investigation include pad printing [36], blade casting [32], spray coating [80], screen printing [81] and inkjet printing [82]. In addition, systematic effort is being directed towards the fabrication of multilayer transducers with a stacked architecture [83, 84]. The emphasis placed by the above-mentioned studies on the fabrication processes and protocols offers great promise for the projection of the manufacturing techniques for DE transducers towards industrial production. However, the final fabrication scenario of DEG PTO systems is still to be studied and research efforts should be oriented towards the understanding of how existing industrial processes could be adapted (or redesigned) for the manufacturing of multilayer membranes at larger scales through continuous/low-cost processes.

6.3 Opportunities and roadmap

DEGs are still an early stage technology, discovered less than 20 years ago. As with many other new technologies, it carries with it several unknowns and challenges, but it is also potentially subject to rapid disruptive innovations that might cause drastic improvements to its already promising performance. Specifically, great opportunities are identified in the development of *new materials* and *new WEC architectures*.

Regarding *materials*, a great potential for the future of DEGs is represented by advances in the field of silicone DEs. Recent studies have demonstrated the possibility of modifying and tailoring the properties of silicone elastomers, thus yielding improved dielectric and mechanical properties. Current efforts are focusing on the synthesis of silicone DEs with higher permittivity and dielectric strength, and with lower elastic modulus [29, 85]. Such improved dielectric properties (ε and E_{BD}) would increase the convertible energy density of DEGs (see Sect. 2.1), while a reduction in

the elastic modulus would limit the need for stiffness compensation mechanisms (e.g., increased hydrodynamic inertia) in coupled DEG-WEC systems (see Sect. 3.3). Based on current trends in material science, the upcoming generation of DE materials might enable the construction of DEG PTOs with convertible power densities that are orders of magnitude larger than those demonstrated to date. The improvement in DEs' permittivity plays a particularly crucial role. Increasing the dielectric constant potentially allows for a reduction in the operating voltage and electric fields, while still guaranteeing large values of the convertible energy densities. This would lead, on the one hand, to a cost reduction of power electronics and, on the other hand, to a significant increase in the DEGs lifetime and reliability. A remarkable milestone has been recently obtained by [86]. That paper describes the synthesis of a novel silicone material with relative dielectric constant above 20 (compared to typical values for silicones of 2-4) and electric breakdown in the order of 80 MV/m (similar to existing silicones).

Regarding *WEC architectures*, in recent years, a trend towards the development of compliant WECs based on soft polymeric materials has emerged. This has led to the investigation of new concepts of attenuators [87], point absorbers [88], and pressure differential devices [89], free from rigid moving parts. Those solutions might, in turn, lead to a benefit in terms of capital costs and reliability. Compared to rigid structures, soft components appear to be more suitable to resist the variable and impulsive wave loads, as they intrinsically exhibit smooth and shock-free structural responses. DEGs enable the application of such a design paradigm not just to the WEC structure, but also to the PTO system. Therefore, thinking beyond the layouts and concepts discussed in this paper, DEGs represent an ideal solution to be paired with a completely new generation of WEC devices based on soft polymeric structures.

Following the deployment of the first medium/large scale DEG PTOs, it is expected that the roadmap towards their application will pursue a gradual increase in complexity. In particular, it is assumed that small/intermediate scale DEG-PTO modules will be first realized for niche market applications (with a few kilowatts of rated power). This will probably be for on-shore installations, which enable fast replacement and low-cost maintenance. Following that, there will be a gradual maturation for near-shore installations at an intermediate power scale (tens/hundreds of kilowatts) and, finally, towards offshore Megawatt scale applications for grid electricity production.

7 Conclusions

This paper provides a detailed review of the results achieved over the last six years of work accomplished by a multidisciplinary team of European researchers on the development of Wave Energy Converters (WECs) equipped with Dielectric Elastomer Generator (DEG) Power-Take-Off (PTO) systems. Following a general introduction on the DEG operating principle and relevant material properties, the paper first describes inflatable DEGs shaped as circular diaphragms (CD-DEGs). This configuration is the most suitable architecture for the implementation of effective PTO systems for Oscillating Water Column (OWC) and Pressure Differential (PD) WECs. A general modelling framework, which relies on electromechanical energy conservation, mechanical degree of freedom reduction and potential flow theory, is then introduced to study the non-linear resonating behaviour of CD-DEG-based WECs. The resulting mathematical models are computationally inexpensive, yet rather accurate, and are suitable for CD-DEG-based WEC design, control and techno-economic assessment. After a discussion on scaling laws for CD-DEG PTO performances, a summary is provided on the major outcomes of the experimental tests conducted so far on small-scale CD-DEG PTOs and on OWCs based on DEGs. The described tests led to a validation of the technology up to a scale of 1:8 in a benign real-sea test-site and to a scale of 1:30 in wave tanks, with a gener-

ated power output of 3.8 W that is the largest ever recorded with a DEG. Moreover, experimental results highlight the effectiveness of the introduced modelling framework for overall system design and control. Following this, the paper identifies DEG lifetime and manufacturing as the most imminent challenges to be addressed in future works, in order to make DEG PTOs an economically affordable solution for the marine energy market. Related to this, recent material discoveries and engineering developments allow to provide a positive outlook on possible future developments of DEG technology. The paper concludes by discussing possible steps to bring CD-DEG-based WECs from small-scale prototypes to full-scale commercial systems.

Acknowledgement

The research leading to these results has received funding from: the European Union Seventh Framework Programme (FP7/2007–2013) under the project PolyWEC (grant agreement No. 309139), from the European Union Horizon 2020 Program, the Project WETFEET (grant agreement No. 646436), from Tuscany Region (Italy) under the project EOLO (FAR FAS 2014-A) and from Wave Energy Scotland WES-PTO Programme under the project Direct Contact Dielectric Elastomer Generator PTO.

References

[1] K. Gunn and C. Stock-Williams, "Quantifying the global wave power resource," *Renewable Energy*, vol. 44, pp. 296–304, 2012.

[2] A. Falcão, "Wave energy utilization: A review of the technologies," *Renewable and sustainable energy reviews*, vol. 14, no. 3, pp. 899–918, 2010.

[3] A. Pecher and J. P. Kofoed, *Handbook of Ocean Wave Energy*. Springer, 2016.

[4] R. Pelrine, R. Kornbluh, Q. Pei, and J. Joseph, "High-speed electrically actuated elastomers with strain greater than 100%," *Science*, vol. 287, no. 5454, pp. 836–839, 2000.

[5] R. Pelrine, R. D. Kornbluh, J. Eckerle, P. Jeuck, S. Oh, Q. Pei, and S. Stanford, "Dielectric elastomers: generator mode fundamentals and applications," in *SPIE's 8th Annual International Symposium on Smart Structures and Materials*. International Society for Optics and Photonics, 2001, pp. 148–156.

[6] S. Shian, J. Huang, S. Zhu, and D. R. Clarke, "Optimizing the electrical energy conversion cycle of dielectric elastomer generators," *Advanced Materials*, vol. 26, no. 38, pp. 6617–6621, 2014.

[7] R. Kaltseis, C. Keplinger, S. J. A. Koh, R. Baumgartner, Y. F. Goh, W. H. Ng, A. Kogler, A. Tröls, C. C. Foo, Z. Suo, and S. Bauer, "Natural rubber for sustainable high-power electrical energy generation," *RSC Advances*, vol. 4, no. 53, pp. 27 905–27 913, 2014.

[8] R. D. Kornbluh, R. Pelrine, H. Prahlad, A. Wong-Foy, B. McCoy, S. Kim, J. Eckerle, and T. Low, "From boots to buoys: promises and challenges of dielectric elastomer energy harvesting," in *Electroactivity in Polymeric Materials*. Springer, 2012, pp. 67–93.

[9] P. Jean, A. Wattez, G. Ardoise, C. Melis, R. Van Kessel, A. Fourmon, E. Barrabino, J. Heemskerk, and J. Queau, "Standing wave tube electro active polymer wave energy converter," in *SPIE Smart Structures and Materials+ Nondestructive Evaluation and Health Monitoring*. International Society for Optics and Photonics, 2012.

[10] B. Scherber, M. Grauer, and A. Köllnberger, "Electroactive polymers for gaining sea power," in *SPIE Smart Structures and Materials+ Nondestructive Evaluation and Health Monitoring*. International Society for Optics and Photonics, 2013.

[11] H. Wille and S. Boureau, "Near shore wec system," Dec. 8 2011, wO2011151693.

[12] G. Moretti, M. Fontana, and R. Vertechy, "Model-based design and optimization of a dielectric elastomer power take-off for oscillating wave surge energy converters," *Meccanica*, vol. 50, no. 11, pp. 2797–2813, 2015.

[13] T. Heath, "A review of oscillating water columns," *Phil. Trans. R. Soc. A*, vol. 370, no. 1959, pp. 235–245, 2012.

[14] G. Neidlein and C. Heintschel, "Wave energy transformer for generator for converting mechanical wave energy into electrical energy in wave energy plant, has electro active polymer foil and is arranged as wave follower in floating body," May 19 2011, dE102009053393 (A1).

[15] R. Vertechy, G. P. P. Rosati, and M. Fontana, "Reduced model and application of inflating circular diaphragm dielectric elastomer generators for wave energy harvesting," *Journal of Vibration and Acoustics*, vol. 137, no. 1, pp. 011 016–1–011 016–9, 2015.

[16] G. Moretti, G. P. R. Papini, M. Righi, D. Forehand, D. Ingram, R. Vertechy, and M. Fontana, "Resonant wave energy harvester based on dielectric elastomer generator," *Smart Materials and Structures*, vol. 27, no. 3, p. 035015, 2018.

[17] G. Moretti, G. P. Rosati Papini, L. Daniele, D. Forehand, D. Ingram, R. Vertechy, and M. Fontana, "Modelling and testing of a wave energy converter based on dielectric elastomer generators," *Proceedings of the Royal Society A*, vol. 475, no. 2222, 2019.

[18] "PolyWEC project web site," http://polywec.org.

[19] "WetFeet project web site," http://http://www.wetfeet.eu/.

[20] "Wave Energy Energy Scotland Website," http://www.waveenergyscotland.co.uk, accessed: 2018-07-31.

[21] "Alternative generation technologies - landscaping study," Wave Energy Scotland, Tech. Rep., 2018.

[22] A. Alessi, E. Bannon, D. Bould, E. De Marchi, P. B. Frigaard, C. G. Soares, J. H. Todalshaug, M. Heward, M. Hofmann, B. Holmes *et al.*, "Workshop on identification of future emerging technologies in the ocean energy sector: Jrc conference and workshop reports," in *JRC Conference and Workshop*. European Commission* Office for Official Publications of the European Union, 2018.

[23] T. McKay, B. O'Brien, E. Calius, and I. Anderson, "Self-priming dielectric elastomer generators," *Smart Materials and Structures*, vol. 19, no. 5, p. 055025, 2010.

[24] S. J. A. Koh, C. Keplinger, T. Li, S. Bauer, and Z. Suo, "Dielectric elastomer generators: how much energy can be converted?" *IEEE/ASME Transactions on mechatronics*, vol. 16, no. 1, pp. 33–41, 2011.

[25] L. Eitzen, C. Graf, and J. Maas, "Cascaded bidirectional flyback converter driving deap transducers," in *IECON 2011-37th Annual Conference on IEEE Industrial Electronics Society*. IEEE, 2011, pp. 1226–1231.

[26] Z. Suo, "Theory of dielectric elastomers," *Acta Mechanica Solida Sinica*, vol. 23, no. 6, pp. 549–578, 2010.

[27] R. Vertechy, M. Fontana, G. Stiubianu, and M. Cazacu, "Open-access dielectric elastomer material database," in *SPIE Smart Structures and Materials+ Nondestructive Evaluation and Health Monitoring*. International Society for Optics and Photonics, 2014, pp. 90 561R–90 561R.

[28] R. Vertechy and M. Fontana, "Electromechanical characterization of a new synthetic rubber membrane for dielectric elastomer transducers," in *SPIE Smart Structures and Materials+ Nondestructive Evaluation and Health Monitoring*. International Society for Optics and Photonics, 2015.

[29] F. B. Madsen, A. E. Daugaard, S. Hvilsted, and A. L. Skov, "The current state of silicone-based dielectric elastomer transducers," *Macromolecular rapid communications*, vol. 37, no. 5, pp. 378–413, 2016.

[30] G. Moretti, M. Fontana, and R. Vertechy, "Modeling and control of lozenge-shaped dielectric elastomer generators," in *ASME 2013 Conference on Smart Materials, Adaptive Structures and Intelligent Systems*. American Society of Mechanical Engineers, 2013.

[31] F. Madsen, L. Yu, P. Mazurek, and A. Skov, "A simple method for reducing inevitable dielectric loss in high-permittivity dielectric elastomers," *Smart Materials and Structures*, vol. 25, no. 7, p. 075018, 2016.

[32] G. Moretti, M. Righi, R. Vertechy, and M. Fontana, "Fabrication and test of an inflated circular diaphragm dielectric elastomer generator based on PDMS rubber composite," *Polymers*, vol. 9, no. 7, p. 283, 2017.

[33] S. Rosset and H. R. Shea, "Flexible and stretchable electrodes for dielectric elastomer actuators," *Applied Physics A*, vol. 110, no. 2, pp. 281–307, 2013.

[34] G. Kovacs, L. Düring, S. Michel, and G. Terrasi, "Stacked dielectric elastomer actuator for tensile force transmission," *Sensors and actuators A: Physical*, vol. 155, no. 2, pp. 299–307, 2009.

[35] B. Chen, Y. Bai, F. Xiang, J.-Y. Sun, Y. Mei Chen, H. Wang, J. Zhou, and Z. Suo, "Stretchable and transparent hydrogels as soft conductors for dielectric elastomer actuators," *Journal of Polymer Science Part B: Polymer Physics*, vol. 52, no. 16, pp. 1055–1060, 2014.

[36] S. Rosset, O. A. Araromi, S. Schlatter, and H. R. Shea, "Fabrication process of silicone-based dielectric elastomer actuators," *Journal of visualized experiments: JoVE*, no. 108, 2016.

[37] H.-Y. Ong, M. Shrestha, and G.-K. Lau, "Microscopically crumpled indium-tin-oxide thin films as compliant electrodes with tunable transmittance," *Applied Physics Letters*, vol. 107, no. 13, p. 132902, 2015.

[38] A. F. Falcão and J. C. Henriques, "Oscillating-water-column wave energy converters and air turbines: A review," *Renewable Energy*, vol. 85, pp. 1391–1424, 2016.

[39] G. Moretti, G. P. Rosati Papini, M. Alves, M. Grases, R. Vertechy, and M. Fontana, "Analysis And Design of an Oscillating Water Column Wave Energy Converter with Dielectric Elastomer Power Take-Off," in *ASME 2015 34th International Conference on Ocean, Offshore and Arctic Engineering*. American Society of Mechanical Engineers, 2015.

[40] R. Vertechy, M. Fontana, G. P. Rosati Papini, and D. Forehand, "In-tank tests of a dielectric elastomer generator for wave energy harvesting," in *SPIE Smart Structures and Materials+ Nondestructive Evaluation and Health Monitoring*. International Society for Optics and Photonics, 2014.

[41] M. S. Semo, "Useful power from ocean waves," Nov. 21 1967, uS Patent 3,353,787.

[42] J. Falnes, *Ocean waves and oscillating systems: linear interactions including wave-energy extraction*. Cambridge University Press, 2002.

[43] G. P. R. Papini, G. Moretti, R. Vertechy, and M. Fontana, "Control of an oscillating water column wave energy converter based on dielectric elastomer generator," *Nonlinear Dynamics*, vol. 92, no. 2, pp. 181–202, 2018.

[44] F. Arena, L. Daniele, V. Fiamma, M. Fontana, G. Malara, G. Moretti, A. Romolo, G. P. Rosati Papini, A. Scialò, and R. Vertechy, "Field Experiments on Dielectric Elastomer Generators integrated on a U-OWC Wave Energy Converter," in *ASME 2018 37th International Conference on Ocean, Offshore and Arctic Engineering*. American Society of Mechanical Engineers, 2018.

[45] J. Henriques, J. Portillo, L. Gato, R. Gomes, D. Ferreira, and A. Falcao, "Design of oscillating-water-column wave energy converters with an application to self-powered sensor buoys," *Energy*, vol. 112, pp. 852–867, 2016.

[46] G. Malara, A. Romolo, V. Fiamma, and F. Arena, "On the modelling of water column oscillations in u-owc energy harvesters," *Renewable Energy*, vol. 101, pp. 964–972, 2017.

[47] M. Fontana, L. Daniele, G. Moretti, F. Damiani, M. Righi, R. Vertechy, B. Teillant, M. Vicente, A. Sarmento, D. Forehand, and D. Ingram, "Wave motion generator based on a dielectric elastomer with stiffness compensation," 28 2018, wO2018116276 (A1).

[48] T. Todorčević, R. van Kessel, P. Bauer, and J. A. Ferreira, "A modulation strategy for wide voltage output in dab-based dc–dc modular multilevel converter for deap wave energy conversion," *IEEE Journal of Emerging and Selected Topics in Power Electronics*, vol. 3, no. 4, pp. 1171–1181, 2015.

[49] G. Moretti, M. Fontana, and R. Vertechy, "Parallelogram-shaped dielectric elastomer generators: analytical model and experimental validation," *Journal of Intelligent Material Systems and Structures*, vol. 26, no. 6, pp. 740–751, 2015.

[50] G. Malara, R. Gomes, F. Arena, J. Henriques, L. Gato, and A. Falcão, "The influence of three-dimensional effects on the performance of U-type oscillating water column wave energy harvesters," *Renewable Energy*, 2017.

[51] H. Goldstein, C. Poole, and J. Safko, *Classical Mechanics - Third Edition*. Addison Wesley, 2001.

[52] A. Babarit, J. Hals, M. Muliawan, A. Kurniawan, T. Moan, and J. Krokstad, "Numerical benchmarking study of a selection of wave energy converters," *Renewable Energy*, vol. 41, pp. 44–63, 2012.

[53] J. Falnes and A. Kurniawan, "Fundamental formulae for wave-energy conversion," *Royal Society open science*, vol. 2, no. 3, p. 140305, 2015.

[54] J. Newman and C.-H. Lee, "Boundary-element methods in offshore structure analysis," *Journal of Offshore Mechanics and Arctic Engineering*, vol. 124, no. 2, pp. 81–89, 2002.

[55] C.-H. Lee and J. N. Newman, "Wamit user manual," *WAMIT, Inc*, 2006.

[56] P. Steinmann, M. Hossain, and G. Possart, "Hyperelastic models for rubber-like materials: consistent tangent operators and suitability for treloar's data," *Archive of Applied Mechanics*, vol. 82, no. 9, pp. 1183–1217, 2012.

[57] A. Pecher, "Experimental testing and evaluation of wecs," in *Handbook of Ocean Wave Energy*, A. Pecher and J. P. Kofoed, Eds. Springer, 2016, ch. 9, pp. 221–260.

[58] W. Sheng and A. Lewis, "Wave energy conversion of oscillating water column devices including air compressibility," *Journal of Renewable and Sustainable Energy*, vol. 8, no. 5, p. 054501, 2016.

[59] A. F. Falcão and J. C. Henriques, "Model-prototype similarity of oscillating-water-column wave energy converters," *International Journal of Marine Energy*, vol. 6, pp. 18–34, 2014.

[60] M. Righi, R. Vertechy, and M. Fontana, "Experimental characterization of a circular diaphragm dielectric elastomer generator," in *ASME 2014 Conference on Smart Materials, Adaptive Structures and Intelligent Systems*. American Society of Mechanical Engineers, 2014.

[61] G. Moretti, G. P. Rosati, M. Fontana, and R. Vertechy, "Hardware in the loop simulation of a dielectric elastomer generator for oscillating water column wave energy converters," in *OCEANS 2015-Genova*. IEEE, 2015, pp. 1–7.

[62] J. B. Shiach, C. G. Mingham, D. M. Ingram, and T. Bruce, "The applicability of the shallow water equations for modelling violent wave overtopping," *Coastal Engineering*, vol. 51, no. 1, pp. 1–15, 2004.

[63] D. Ingram, R. Wallace, A. Robinson, and I. Bryden, "The design and commissioning of the first, circular, combined current and wave test basin." *Flow3d. com*, 2014.

[64] F. Arena and G. Barbaro, "The natural ocean engineering laboratory, noel, in reggio calabria, italy: A commentary and announcement," *Journal of Coastal Research*, vol. 29, no. 5, pp. vii–x, 2013.

[65] "EAP material and product manufacturers," https://ndeaa.jpl.nasa.gov/nasa-nde/lommas/eap/EAP-material-n-products.htm.

[66] D. Magagna, R. Monfardini, and A. Uihlein, "Ocean energy in europe," *International Marine Energy Journal*, vol. 1, no. 1 (Aug), pp. 1–7, 2018.

[67] A. Pecher and R. Costello, *Techno-Economic Development of WECs*. Springer, 2016, ch. 4, pp. 81–100.

[68] B. Teillant, M. Vicente, G. P. Rosati Papini, G. Moretti, R. Vertechy, M. Fontana, K. Monk, and M. Alves, "Techno-economic comparison between air turbines and dielectric elastomer generators as power take-off for oscillating water column wave energy converters," in *EWTEC 2014 European Wave and Tidal Energy Conference Series*, 2014.

[69] E. S. Rubin, I. M. Azevedo, P. Jaramillo, and S. Yeh, "A review of learning rates for electricity supply technologies," *Energy Policy*, vol. 86, pp. 198 – 218, 2015. [Online]. Available: http://www.sciencedirect.com/science/article/pii/S0301421515002293

[70] A. Uihlein and D. Magagna, "Wave and tidal current energy – a review of the current state of research beyond technology," *Renewable and Sustainable Energy Reviews*, vol. 58, pp. 1070 – 1081, 2016. [Online]. Available: http://www.sciencedirect.com/science/article/pii/S1364032115016676

[71] W. Mars and A. Fatemi, "Factors that affect the fatigue life of rubber: a literature survey," *Rubber Chemistry and Technology*, vol. 77, no. 3, pp. 391–412, 2004.

[72] P.-Y. Le Gac, M. Arhant, P. Davies, and A. Muhr, "Fatigue behavior of natural rubber in marine environment: Comparison between air and sea water," *Materials & Design (1980-2015)*, vol. 65, pp. 462–467, 2015.

[73] R. D. Kornbluh, R. Pelrine, Q. Pei, R. Heydt, S. Stanford, S. Oh, and J. Eckerle, "Electroelastomers: applications of dielectric elastomer transducers for actuation, generation, and smart structures," in *SPIE's 9th Annual International Symposium on Smart Structures and Materials*. International Society for Optics and Photonics, 2002, pp. 254–270.

[74] C. A. de Saint-Aubin, S. Rosset, S. Schlatter, and H. Shea, "High-cycle electromechanical aging of dielectric elastomer actuators with carbon-based electrodes," *Smart Materials and Structures*, vol. 27, no. 7, p. 074002, 2018.

[75] R. Kornbluh, A. Wong-Foy, R. Pelrine, H. Prahlad, and B. McCoy, "Long-lifetime all-polymer artificial muscle transducers," *MRS Online Proceedings Library Archive*, vol. 1271, 2010.

[76] C. Yi, L. Agostini, M. Fontana, G. Moretti, and R. Vertechy, "On the lifetime performance of a styrenic rubber membrane for dielectric elastomer transducers," in *ASME 2018 Conference on Smart Materials, Adaptive Structures and Intelligent Systems*. American Society of Mechanical Engineers, 2018.

[77] Y. Chen, L. Agostini, G. Moretti, G. Berselli, M. Fontana, and R. Vertechy, "Fatigue life performances of silicone elastomer membranes for dielectric elastomer transducers: preliminary results," in *SPIE Smart Structures and Materials+ Nondestructive Evaluation and Health Monitoring*. International Society for Optics and Photonics, 2019.

[78] D. V. Rosato, *Plastics processing data handbook*. Springer Science & Business Media, 2012.

[79] L. W. McKeen, *Film properties of plastics and elastomers*. William Andrew, 2017.

[80] O. Araromi, A. Conn, C. Ling, J. Rossiter, R. Vaidyanathan, and S. Burgess, "Spray deposited multilayered dielectric elastomer actuators," *Sensors and Actuators A: Physical*, vol. 167, no. 2, pp. 459–467, 2011.

[81] B. Fasolt, M. Hodgins, G. Rizzello, and S. Seelecke, "Effect of screen printing parameters on sensor and actuator performance of dielectric elastomer (de) membranes," *Sensors and Actuators A: Physical*, vol. 265, pp. 10–19, 2017.

[82] D. McCoul, S. Rosset, S. Schlatter, and H. Shea, "Inkjet 3d printing of uv and thermal cure silicone elastomers for dielectric elastomer actuators," *Smart Materials and Structures*, vol. 26, no. 12, p. 125022, 2017.

[83] T. G. McKay, S. Rosset, I. A. Anderson, and H. Shea, "Dielectric elastomer generators that stack up," *Smart Materials and Structures*, vol. 24, no. 1, p. 015014, 2014.

[84] Z. Li, M. Sheng, W. Minqing, D. Pengfei, B. Li, and H. Chen, "Stacked dielectric elastomer actuator (sdea): casting process, modeling and active vibration isolation," *Smart Materials and Structures*, 2018.

[85] P. Caspari, S. J. Dünki, F. A. Nüesch, and D. M. Opris, "Dielectric elastomer actuators with increased dielectric permittivity and low leakage current capable of suppressing electromechanical instability," *Journal of Materials Chemistry C*, vol. 6, no. 8, pp. 2043–2053, 2018.

[86] Y. Sheima, S. J. Dünki, F. Nüesch, and D. M. Opris, "Dielectric elastomer actuators operated below 300 v," in *International conference on Electromechanically Active Polymer Transducers & Artificial muscles, Lyon France 5-6 June 2018.* EUROEAP, 2018, pp. 1–2.

[87] F. Farley, R. Rainey, and J. Chaplin, "Rubber tubes in the sea," *Phil. Trans. R. Soc. A*, vol. 370, no. 1959, pp. 381–402, 2012.

[88] A. Kurniawan, J. Chaplin, D. Greaves, and M. Hann, "Wave energy absorption by a floating air bag," *Journal of Fluid Mechanics*, vol. 812, pp. 294–320, 2017.

[89] S. Ryan, C. Algie, G. J. Macfarlane, A. N. Fleming, I. Penesis, A. King *et al.*, "The bombora wave energy converter: A novel multi-purpose device for electricity, coastal protection and surf breaks," in *Australasian coasts & ports conference 2015: 22nd Australasian coastal and ocean engineering conference and the 15th Australasian port and harbour conference.* Engineers Australia and IPENZ, 2015, p. 541.

APPENDIX - Application of the modelling approach to OWC and PD cases

This appendix provides examples of application of the general equation of motion for DEG-WEC systems (Eq. (11)) to two specific layouts of the OWC and PD WECs.

OWC with CD-DEG PTO

We consider a square-plan fixed OWC collector with the geometry and dimensions shown in Fig. 7(a). The collector has the bottom surface open towards the sea environment. The surface-piercing air chamber holds multiple CD-DEGs as the PTO.
We use the displacement z (positive upwards) of the water column from the SWL as the generalised coordinate: $q = z$.
In the equilibrium condition, $z = 0$, the CD-DEGs are flat ($h = 0$) and the air pressure equals the atmospheric pressure, $p_0 = p_{atm}$.
Assuming that the water column behaves as a rigid piston (i.e., particles velocity is uniform throughout the different collector sections), the kinetic energy associated with the fluid control volume is:

$$\mathcal{E}_k = \frac{1}{2}\rho c w (h_i + z)\dot{z}^2, \tag{23}$$

where c and w are the collector breadth and width respectively. The control water volume inertia is thus

$$M_q = \rho c w (h_i + z), \tag{24}$$

and it depends on z.
Taking the SWL as the zero-potential energy plane, the gravitational energy of the water volume reads as:

$$\mathcal{E}_g = \mathcal{E}_{g,0} + \frac{1}{2}\rho c w g z^2, \tag{25}$$

where $\mathcal{E}_{g,0}$ is a parameter accounting for the gravitational energy of the constant water volume below the SWL.
As the water cross-section is constant, $v_i = \dot{z}$ and $\kappa_i = 1$.
The air chamber volume relates to z and to the volume subtended by the CD-DEGs as follows:

$$\Omega_a = \Omega_0 - cwz + N_D \Omega_c, \tag{26}$$

thus, its derivative with respect to z is

$$\frac{\mathrm{d}\Omega_a}{\mathrm{d}z} = -cw + N_D \frac{\Omega_c}{\mathrm{d}z}. \tag{27}$$

For the relative air pressure, $p = p_a - p_{atm}$, Eq. (21) applies. Combining Eqs. (26-27) and Eq. (21) provides the values of air pressure p, CD-DEG subtended volume Ω_c (and, thus, h) and air chamber volume Ω_a at given z and V.

Using Eqs. (24-21) in Eq. (11) yields the following equation of motion for the OWC:

$$\rho c (h_i + z)\ddot{z} + \rho c g z + cp = c p_w, \tag{28}$$

in which the contribution of the CD-DEG is expressed by the relative pressure p (given by Eq. (21)). The wave pressure p_w is calculated according to the procedure described in Sect. 4.2, whereas the expressions of $\mathcal{E}_{m,s}$ and C as functions of Ω_c can be inferred as explained in Sect. 4.3.

PD WEC with CD-DEG PTO

We consider the PD WEC shown in Fig. 7(b). The device holds a single CD-DEG PTO horizontally mounted on a fixed submerged air chamber. We set $q = \Omega_c$ as the generalised coordinate.
The CD-DEG cap volume in the equilibrium configuration is indicated by $\Omega_{c,0}$. In that configuration, the equilibrium air pressure is p_0.
The potential gravitational energy of the water control volume is:

$$\mathcal{E}_g = \mathcal{E}_{g,0} + \rho g \Omega_c \zeta_c, \tag{29}$$

where $\mathcal{E}_{g,0}$ is a constant accounting for the gravitational energy of the water volume above the CD-DEG base plane, and ζ_c is the coordinate of the centre of mass of the water cap comprised between the DEG shell and its base plane in the $\xi - \zeta$ reference system shown in Fig. 7 (notice that $\zeta_c < 0$). The coordinate ζ_c can be uniquely related to Ω_c knowing the geometry of the deformed CD-DEG.
Based on the mass flow balance in the control volume, the inlet water velocity is $v_i = \dot{\Omega}_c / S_i$, therefore $k_i = S_i^{-1}$.
The air chamber volume is $\Omega_a = \Omega_0 + \Omega_{c,0} - \Omega_c$ and it equals Ω_0 in equilibrium conditions.
The calculation of the generalised hydrostatic inertia is non-trivial, as it requires knowledge of the water velocity field within the water control volume. As suggested in Sect. 4.2, that term can be conveniently calculated (in a linearised form, $M_{q,0} = M_q(\Omega_{c,0})$) via the BEM. The quadratic term in Eq. (11) is neglected, as discussed in Sect. 4.1.

The mentioned assumptions lead to the following form for the PD WEC equation of motion:

$$M_{q,0}\ddot{\Omega}_c + \rho g \left(\zeta_c + \Omega_c \frac{\mathrm{d}\zeta_c}{\mathrm{d}\Omega_c} \right) + p + \frac{\mathrm{d}\mathcal{E}_{m,s}}{\mathrm{d}\Omega_c} - \frac{V^2}{2} \frac{\mathrm{d}C}{\mathrm{d}\Omega_c} = p_w \tag{30}$$

where $p = p_a - p_{atm}$ is the relative air pressure, calculated by feeding the expression for Ω_a into Eq. (3). As in the OWC example, the wave pressure term can be calculated using the approach proposed in Sect. 4.2, and the terms related to the CD-DEG are calculated as discussed in Sect. 4.3.

It is worth noticing that the PD WEC modelling approach presented so far is a strong simplification, based on several assumptions (above all, the reduction of the CD-DEG kinematics to one degree of freedom). Despite its simplicity, this approach provides a convenient and computationally inexpensive tool for preliminary analysis. Moreover, building upon the proposed energetic formulation, it is possible to extend the presented model to a multiple-degree-of-freedom model, describing the CD-DEG deformation as a superposition of deformed modal shapes, and writing a set of equations of motions for the different degrees of freedom accordingly.